Intracellular Maturation and Transport of the SV5 Type II Glycoprotein Hemagglutinin-Neuraminidase: Specific and Transient Association with GRP78-BiP in the Endoplasmic Reticulum and Extensive Internalization from the Cell Surface

Davis T. W. Ng, Rick E. Randall,* and Robert A. Lamb

Department of Biochemistry, Molecular Biology and Cell Biology, Northwestern University, Evanston, Illinois 60208-3500; and *Department of Biochemistry and Microbiology, University of St. Andrews, St. Andrews, Fife KY16 9AL Scotland

Abstract. The hemagglutinin-neuraminidase (HN) glycoprotein of the paramyxovirus SV5 is a type II integral membrane protein that is expressed at the infected cell surface. The intracellular assembly and transport of HN in CV1 cells was examined using conformation-specific HN mAbs and sucrose density sedimentation analysis. HN was found to oligomerize with a $t_{½}$ of 25–30 min and these data suggest the oligomer is a tetramer consisting primarily of two noncovalently associated disulfide-linked dimers. As HN oligomers could be found that were sensitive to endoglycosidase H digestion and oligomers formed in the presence of the ER to the Golgi complex transport inhibitor, carbonylcyanide *m*-chlorophenylhydrazone (CCCP), these data are consistent with HN oligomerization occurring in the ER. Unfolded or immature HN molecules that could not be recognized by conformation-specific antibodies were found to specifically associate with the resident ER protein GRP78-BiP. Immunoprecipitation of BiP-HN complexes with an immunoglobulin heavy-chain binding protein (BiP) antibody indicated that newly synthesized HN associated and dissociated from GRP78-BiP ($t_{½}$ 20–25 min) in an inverse correlation with the gain in reactivity with a HN conformation-specific antibody, suggesting that the transient association of GRP78-BiP with immature HN is part of the normal HN maturation pathway. After pulse-labeling of HN in infected cells, it was found that HN is rapidly turned over in cells ($t_{½}$ 2–2.5 h). This led to the finding that the vast majority of HN expressed at the cell surface, rather than being incorporated into budding virions, is internalized and degraded after localization to endocytic vesicles and lysosomes.

VIRAL envelope glycoproteins have frequently been used as model systems in the study of transport in the exocytic pathway e.g., the hemagglutinin protein (HA)[1] of influenza virus and the glycoprotein (G) of VSV. Both HA and G are class I integral membrane proteins that are oriented in the ER with an NH_2-terminal ectodomain and a COOH-terminal cytoplasmic tail (reviewed in reference 57). Assembly into noncovalently linked homotrimers is thought to occur in the ER before transport through the exocytic pathway (5, 6, 14) and this assembly is fairly rapid ($t_{½}$ 7–10 min for HA [14] and $t_{½}$ 6–8 min for G [7]). It has been proposed from studies using wild-type and mutant molecules that do not fold correctly that native folding and oligomerization may be a prerequisite for transport out of the ER and thus it may be a rate-limiting step (14, 28, reviewed in reference 57). The exact nature of the signals and macromolecular interactions which are necessary for this apparent requirement are unknown although it has been observed that the resident ER protein, immunoglobulin heavy-chain binding protein (BiP) (18), is associated with unfolded and malfolded mutant molecules of HA (14). However, it has not been determined if the association of BiP with HA is part of the normal maturation pathway of HA or if BiP is only involved with improperly folded molecules. Evidence in support of a role of BiP in the maturation and assembly of proteins came from studies using lymphoid-derived cell lines. BiP was found to be associated with Ig heavy chains in nonsecreting pre-B cell lines and to Ig precursors in secreting hybridomas and myelomas but not with the completely assembled protein (H_2L_2) (1, 20). It was hypothesized that BiP prevented the transport of incompletely assembled Ig chains, insuring that only fully assembled proteins were transported (1, 20).

Recently, BiP has been identified as identical to the glucose-regulated protein, GRP78 (22, 43), a highly conserved cellular protein (here designated GRP78-BiP) that is a mem-

1. *Abbreviations used in this paper*: BiP, binding protein; CCCP, carbonylcyanide *m*-chlorophenylhydrazone; F, fusion protein; G, glycoprotein; HA, hemagglutinin protein; HN, hemagglutinin-neuraminidase; MNT buffer, 20 mM morpholino-ethanesulfonic acid; p.i., postinfection.

ber of the HSP70 family of stress-related proteins. GRP78-BiP has been found in all cell types examined and synthesis of GRP78-BiP can be stimulated by various perturbations such as glucose deprivation, inhibition of glycosylation, interference of intracellular calcium concentrations, infection with paramyxoviruses such as SV5, and the presence of malfolded proteins in the ER (10, 27, 50, 54, 69). Although the function of GRP78-BiP is unclear, it has been proposed to have a role in the folding and assembly of proteins in the exocytic pathway (1, 14, 20, 21, 44, 47), to mark aberrantly folded proteins destined for degradation (9, 25, 34), or to aid in solubilizing aggregated proteins during periods of stress (43).

Viral envelope proteins have also been used as models to study aspects of the endocytic pathway. When VSV G is expressed in cells transfected with recombinant DNA molecules it is slowly internalized from and returned to the cell surface in a process similar to that found for recycling cellular receptor molecules (17, 37, 51, 58). In addition, when G is directly implanted on the apical surface of polarized cells, it is internalized and transported to the basolateral surface, where it is normally resident (37, 51). In contrast, influenza HA normally accumulates in a stable manner at the cell surface and is not internalized. However, when the HA cytoplasmic tail was replaced with that of VSV G, HA became internalized, suggesting that an internalization signal lies in the cytoplasmic tail. It has also been shown with HA that a properly positioned tyrosine residue is required in the cytoplasmic tail for recycling to occur (31), as was hypothesized for the LDL receptor molecule (15). Although these studies are few in number, they have shown that well-characterized viral membrane glycoproteins can also be useful model systems for understanding processes in the endocytic pathway.

In paramyxovirus-infected cells two virus-specific integral membrane glycoproteins, the hemagglutinin-neuraminidase (HN) and the fusion protein (F) are synthesized. These proteins are synthesized on membrane-bound polysomes, and are inserted into the ER and transported via the exocytic pathway to the cell surface (reviewed in reference 53). Like influenza HA and VSV G, the F glycoprotein is a class I glycoprotein inserted into membranes with a NH_2-terminal ectodomain, whereas HN is a class II integral membrane protein which has an uncleaved NH_2-terminal signal/anchor domain and a COOH-terminal ectodomain (23, 24, 45). Both glycoproteins are incorporated into virions where HN mediates receptor-binding activities (hemagglutination) and F mediates membrane fusion activity with target cells (61, 62). In addition, HN has a receptor-destroying activity (neuraminidase) that is thought to be important in the release of progeny virus from cells (reviewed in reference 4).

In this study, we have examined the folding, oligomeric assembly, and transport in the exocytic pathway of the SV5 HN glycoprotein as a model class II integral membrane protein. These experiments were greatly facilitated by using antibodies specific for different conformational states of the protein. We provide data that indicate that GRP78-BiP specifically and transiently associates with HN as part of the normal maturation pathway. Additionally, we unexpectedly find that HN is rapidly turned over in cells and this is because once HN is expressed at the cell surface it is internalized and localized to endosomal vesicles and lysosomes.

Materials and Methods

Cells and Virus

The TC7 clone of CV1 cells and a variant of the Madin-Darby bovine kidney cell line (MDBK) were grown and maintained in DME supplemented with 10% FCS. The W3A strain of SV5 was grown in MDBK monolayer cultures as described previously (45).

Antibodies

The purified IgG fraction of rabbit polyclonal antisera raised against purified SV5 HN was that used previously (39, 40). The isolation of mouse mAbs specific to HN (HN-1b and HN-4b) and to F (F-1a) has been described previously (56). mAbs HN-1b and HN-4b were shown to bind different antigenic sites on HN by radioimmune competition assay (56). A rat mAb (anti-BiP), specific for the cellular heavy-chain binding protein (BiP), was kindly provided by Drs. Linda Hendershot (St. Jude Children's Research Hospital, Memphis, TN) and John F. Kearney, (University of Alabama, Birmingham, AL) (1). All antisera described were titrated using an immunoprecipitation assay and were then used in all experiments under conditions of antibody excess.

Viral Infection and Metabolic Labeling of Cells

SV5-infected CV1 cells were used in all the biochemical studies. CV1 cells were washed in PBS and infected with SV5 at ~20 plaque-forming units/cell in DME containing 0.5% BSA for 1 h at 37°C. Cells were washed with DME and the medium was replaced with DME supplemented with 2% FCS. Infected cells were maintained at 37°C in an atmosphere containing 5% CO_2. Metabolic labeling of cells was typically carried out 14–16 h after infection (p.i.). In protocols in which a short radioactive labeling period was required followed by incubations in unlabeled medium (cold chase), cells were washed twice with PBS, and incubated with cysteine- and methionine-deficient DME (DME cys^-/met^-) for 30 min. Cells were then labeled with 50–100 μCi Tran[^{35}S]-label (ICN Radiochemicals, Irvine, CA) in DME cys^-/met^- and incubated at 37°C for the duration of the pulse. A cold chase was initiated by removal of the labeling medium and immediately replacing it with prewarmed chase medium consisting of DME, 2 mM unlabeled cysteine and methionine, and 2% FCS. The chase period was terminated by washing cells in ice-cold PBS followed with lysis in an appropriate detergent buffer for immunoprecipitation. In protocols where steady state labeling was required, cells were washed once in DME cys^-/met^- and incubated in labeling medium that consisted of a 1:5 mix of DME to DME cys^-/met^- supplemented with 2% FCS and 100 μCi/ml [^{35}S]methionine (Amersham Corp., Arlington Heights, IL).

Immunoprecipitation, SDS-PAGE, and Quantitation of Autoradiograms

Immunoprecipitation of HN from labeled infected-cell lysates was performed essentially as described unless where indicated (30). SDS-PAGE was done as described (29). Autoradiograms were quantitated by scanning densitometry on variable exposures of each gel to assure being within the linear range of the film. Densitometry and integration was performed as described (23).

Immunoprecipitation of proteins from sucrose gradient fractions was done by diluting fractions eightfold with 1% NP-40, 0.05% SDS, 50 mM Tris pH 7.4, and 150 mM NaCl (dilution buffer). The appropriate antibody was then added and samples incubated at 4°C for 3 h. 30 μl of a 1:1 slurry of *Staphylococcus aureus* protein A-agarose beads (Calbiochem-Behring Corp., La Jolla, CA) were then added and rocked for 60 min at 4°C to precipitate antibody-antigen complexes. The beads were then washed five times in dilution buffer and once in nondetergent wash buffer (150 mM NaCl, 50 mM Tris pH 7.4, and 5 mM EDTA) before the complexes were boiled for 5 min in SDS-PAGE sample loading buffer.

Coprecipitation of HN/GRP78-BiP was done under ATP-depleting conditions. Radioactively labeled cells were washed once in ice-cold PBS and lysed in 50 mM Tris pH 7.4, 150 mM NaCl, and 1% Triton X-100 (TNT buffer) containing 10 mM glucose and 2 IU hexokinase (Calbiochem-Behring Corp.). Immunoprecipitation was then carried out as described above except that immune complexes were washed in TNT buffer and all steps were performed at 0–4°C.

Serial immunoprecipitations were done as described above through the point of incubation of antigen-antibody complexes with protein A-agarose beads. The beads were pelleted by centrifugation and the supernatant transferred to a second tube. The beads were then washed with 50 μl of TNT buffer and this wash supernatant was pooled with the previous supernatant. The appropriate antibody was then added to the combined supernatants in the second tube and the procedure repeated as many times as required. Protein A-agarose beads containing bound immune complexes from the serial immunoprecipitations were washed with wash buffer and prepared for SDS-PAGE as described above.

Sucrose Density Gradient Sedimentation Analysis of HN Oligomers

The procedure used to analyze the rate of HN oligomerization was modified from that described (5). SV5-infected CV1 cells (60-mm plates) were pulse labeled for 5 min with Tran[^{35}S]-label and incubated with chase medium for varying times. Cells were then lysed in 0.5 ml detergent buffer (20 mM morpholino-ethanesulfonic acid, 30 mM Tris, 100 mM NaCl [MNT buffer] pH 5.0 and 1% Triton X-100) and 1% aprotinin. Nuclei and cell debris were removed by centrifugation for 10 min in a microfuge and the lysate supernatant was layered over the top of a continuous 7.5–22.5% wt/vol sucrose/MNT pH 5.0/0.1% Triton X-100 gradient that overlaid a 0.75-ml 60% sucrose cushion. The final volume was 12 ml. Gradients were centrifuged at 38,000 rpm at 20°C for 20 h in a rotor (model SW41; Beckman Instruments, Inc., Palo Alto, CA). 24 0.5-ml fractions were collected dropwise from the bottom of each gradient by puncturing the bottom of the tube. Aliquots from alternate fractions were then taken for immunoprecipitation, as described above.

Endoglycosidase H Digestion

HN was immunoprecipitated from infected-cell lysates as described above and released from immune complexes by boiling in 10 mM Tris pH 7.4/0.4% SDS. An equal volume of 0.1 M Na-citrate (pH 5.3) and 1 mU of Endo H (Boehringer Mannheim Biochemicals, Indianapolis, IN) was then added and the samples were incubated for 24 h at 37°C. The reaction was terminated by the addition of SDS-PAGE sample loading buffer.

Carbonylcyanide m-Chlorophenylhydrazone Treatment of Cells

SV5-infected cells were pulse-labeled for 10 min as described above and immediately washed in cold PBS before addition of prechilled chase media containing 50 μg/ml carbonylcyanide *m*-chlorophenylhydrazone (CCCP) (Sigma Chemical Co., St Louis, MO). After a 10-min incubation at 4°C, the cells were warmed to 37°C and incubated for 2 h before lysis.

Indirect Immunofluorescence Microscopy

Coverslips of SV5-infected CV1 cells were prepared for cell surface staining by fixing the cells in PBS containing 0.5% methanol-free formaldehyde (Polysciences, Inc., Warrington, PA) for 5 min at room temperature. For intracellular staining, the cells were formaldehyde fixed and permeabilized in acetone for 60 s at −20°C. Ascites fluids containing mAbs HN-1b and F-1a were diluted 1:1,000 in PBS/1% BSA for localization of the HN and F proteins. Binding conditions and incubation with fluorescein-labeled second antibody was done as described previously (46).

To assay for the internalization of surface bound antibody, SV5-infected CV1 cells were shifted to 4°C. mAbs HN-1b or F-1a were added to the live cells and incubated for 30 min at 4°C. Cells were washed extensively in cold PBS to remove unbound antibody and then prewarmed (37°C) DME supplemented with 2% FCS was added and cells were incubated at 37°C. For chloroquine treatment, cells were preincubated for 2 h in medium containing 100 μM chloroquine before addition of antibody and were maintained in the same medium after the temperature shift. At various times following the temperature shift cells were fixed, or fixed and permeabilized, as described above. FITC-conjugated goat anti-mouse antibody (Organon Technica Corp., West Chester, PA) was then added to detect the bound antibody. Photomicroscopy was performed using epifluorescent optics on an Axiophot (Carl Zeiss, Inc., Thornwood, NY) microscope.

Results

Rate of Oligomerization of HN

The HN integral membrane glycoprotein of paramyxoviruses is thought to be a homotetramer. Cross-linking studies combined with the use of nonreducing gels indicated that the HN protein consists of disulfide-linked dimers that form either noncovalently linked tetramers or disulfide-linked tetramers (36). In electron micrographs of purified HN, four subunits forming a homotetramer could be readily identified (65).

To investigate the rate of oligomerization of HN, SV5-infected cells were pulse-labeled for 5 min with Tran[^{35}S]-label and incubated for varying periods from 0–60 min in unlabeled chase medium. The oligomeric form of HN was then analyzed by sucrose density gradient centrifugation. Cell lysis buffers and sucrose density gradient solutions were adjusted to pH 5.0 (approximately the pH optimum of the HN neuraminidase activity [62]), because at higher pH the HN oligomer partially dissociated under the centrifugation conditions used (data not shown). Fractions were collected from the bottom of the gradients and alternate fractions were immunoprecipitated with the polyclonal HN antibody and the polypeptides were analyzed by SDS-PAGE. Immediately after the labeling period, HN was found in a slow sedimenting peak (Fig. 1 *A*, fractions 12–16). After 30 min of chase period, approximately half of HN was found in a faster sedimenting form (fractions 6–8). By 60 min, >90% of HN had been converted to this faster sedimenting form. In a parallel gradient, the trimeric influenza virus HA had a similar rate of sedimentation to oligomeric HN (data not shown). This analysis suggests HN is assembled into a higher order structure and this process has a $t_{½}$ of ~25–30 min. To gain further insight into the nature of the oligomeric form, immunoprecipitated HN was analyzed under nonreducing conditions on SDS-PAGE (Fig. 1 *B*). SV5 HN from the slower sedimenting peak (fractions 14–16) was found to migrate on gels with a similar but slightly altered mobility as compared with reduced monomeric HN due to intramolecular disulfide bonds. SV5 HN from the faster sedimenting form (fractions 6–8) was found on gels to consist of two species, disulfide-linked dimers and tetramers (Fig. 1 *B*, HN_2 and HN_4), suggesting that this species on the gradient is a homotetramer consisting of pairs of disulfide-linked dimers that sometimes form a disulfide-linked tetramer. Although this does not formally prove that HN of SV5 is a tetramer, for purposes of discussion, this will be assumed to be the case. The oligomerization rate for SV5 HN is fairly slow as compared to that found for influenza virus HA or VSV G ($t_{½}$ 7–10 and 6–8 min, respectively) (14, 5) but even so, it was not possible to distinguish between the rate of formation of the oligomer and the rate of formation of the intermolecular disulfide bonds.

Characterization of mAbs as Reagents to Detect Steps in the Folding and Oligomerization of HN

In several other studies on the intracellular transport of glycoproteins, extensive use has been made of mAbs to probe the folded state of the protein (5, 6, 14, 42, 70, 72). To search for mAbs that could recognize conformation-specific forms of HN, a panel of mAbs prepared to SV5 HN (56) was

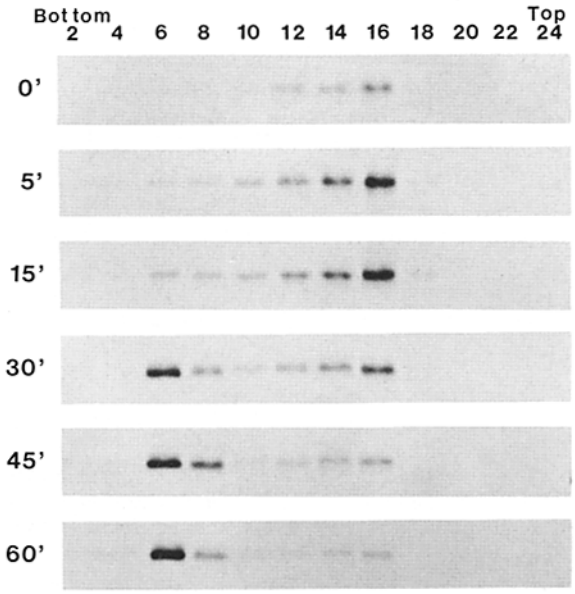

Figure 1. Kinetics of SV5 HN oligomerization. SV5-infected CV1 cells at 16 h p.i. were pulse-labeled for 5 min with Tran[^{35}S]-label. The cells were then incubated for varying periods in chase medium containing unlabeled cysteine and methionine and lysed in Triton X-100. The lysates were then subjected to sucrose velocity sedimentation on 7.5–22.5% wt/vol sucrose gradients at 20°C for 20 h at 38,000 rpm. Fractions were collected from the bottom of each gradient and aliquots from alternate fractions were immunoprecipitated with HN polyclonal antisera and analyzed by SDS-PAGE. (*A*) Samples treated with the reducing agent DTT. Times after the labeling period are indicated. (*B*) Samples electrophoresed under nonreducing conditions (*−DTT*). The positions of monomeric (HN_1), dimeric (HN_2), and tetrameric (HN_4) forms of HN are indicated. Times after the labeling period are indicated.

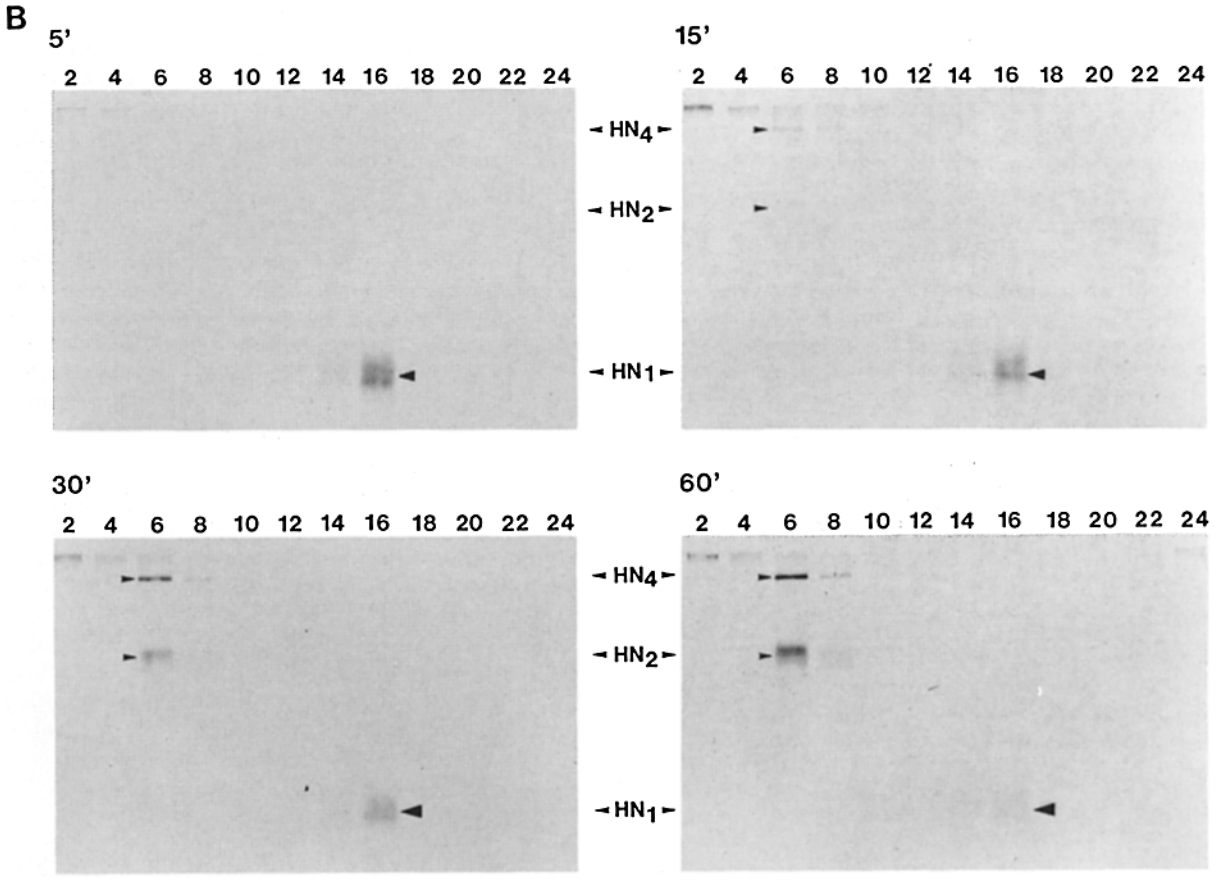

screened. SV5-infected cells were pulse-labeled for 5 min with Tran[^{35}S]-label and chase medium was added for varying periods. The reactivity of the mAbs with HN at different time points was tested by immunoprecipitating samples with the polyclonal HN antibody or with each of the mAbs and analyzing the polypeptides on SDS-PAGE under reducing and nonreducing conditions. An example of the time course of reactivity of HN to a polyclonal antisera and two mAbs

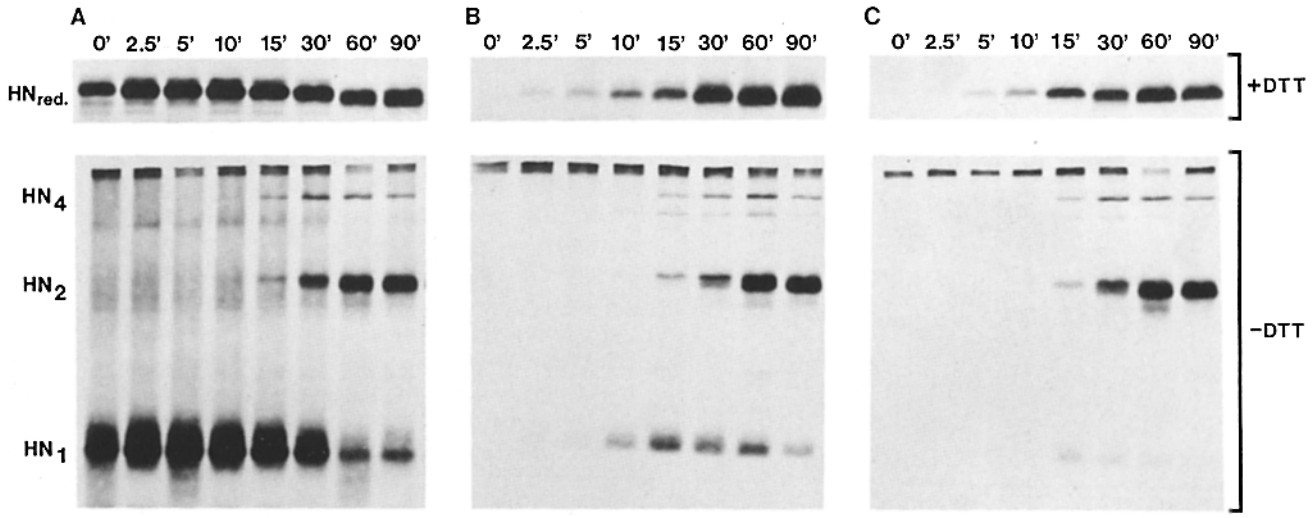

Figure 2. Time course of reactivity of antibodies with HN. SV5-infected CV1 cells were pulse-labeled at 14 h p.i. with Tran[^{35}S]-label for 5 min and incubated for the times indicated in chase medium containing unlabeled cysteine and methionine and lysed in RIPA buffer (30). Aliquots from each time point were used for immunoprecipitation with the different antisera. Following binding of immune complexes to protein A-containing agarose beads, the samples were analyzed by SDS-PAGE either in the presence (*+DTT*) or absence (*−DTT*) of DTT. (*A*) Immunoprecipitation with polyclonal HN antiserum that recognizes all forms of HN. (*B*) Immunoprecipitation with mAb HN-1b. (*C*) Immunoprecipitation with mAb HN-4b.

is shown in Fig. 2. The x-ray films were deliberately overexposed to show the differences in reactivity. The polyclonal HN antibody was capable of immunoprecipitating monomeric HN immediately after the 5-min labeling period (Fig. 2 *A*) but the disulfide-linked dimers (and tetramers) did not begin to form for 15 min after the labeling period. The changes in mobility of HN with increasing period of chase (Fig. 2 *A*, +DTT) reflect carbohydrate trimming and for the unreduced monomeric HN they also reflect the formation of intramolecular disulfide bonds (Fig. 2 *A*, −DTT). When the mAbs were used to immunoprecipitate HN from the same cell lysates neither antibody HN-1b nor HN-4b immunoprecipitated HN immediately after the 5-min pulse period. After 2.5 min of chase, antibody HN-1b began to gain reactivity to HN and after 5 min antibody HN-4b began to gain reactivity to HN (+DTT, *B* and *C*). Reactivity of both mAbs to HN increased with extended times of chase period and by 60 min the amount of HN immunoprecipitated reached similar levels to that precipitated by the polyclonal HN antibody. When the samples were analyzed under nonreducing conditions on gels (Fig. 2, −DTT) the difference between the specificity of the mAbs became clearer. Antibody HN-1B recognized monomeric HN at times (2.5–15 min) before the dimer had formed, whereas antibody HN-4b showed nearly exclusive reactivity with the dimer (Fig. 2 *C*). Thus, the polyclonal HN antibody can recognize all forms of HN, mAb HN-1b recognizes an epitope that forms in the monomer and is maintained in the disulfide-linked dimer and HN-4b has almost exclusive reactivity with the dimeric (and tetrameric) form. Because the formation of intermolecular disulfide

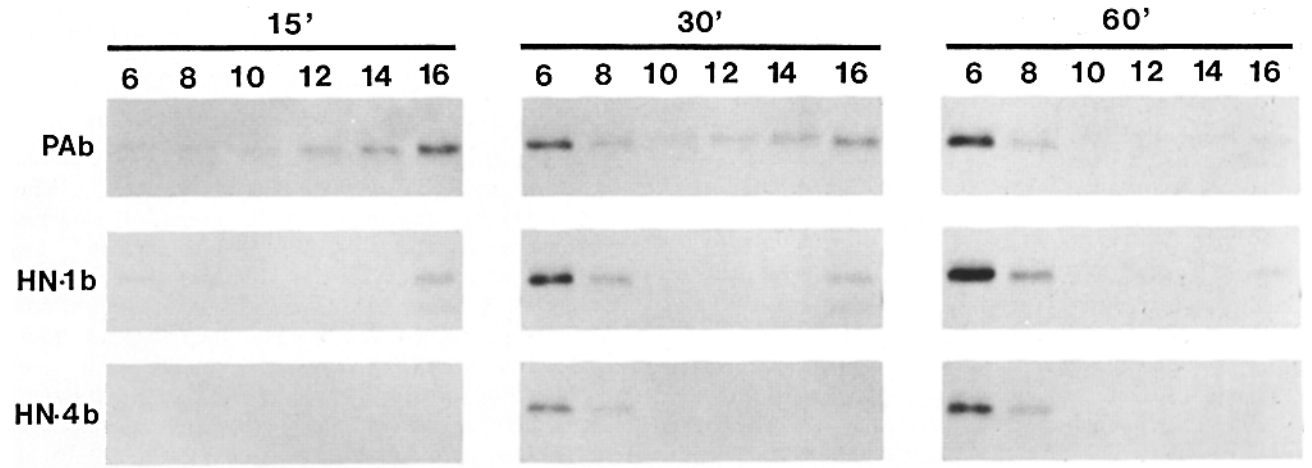

Figure 3. Reactivity of monoclonal antibodies to monomeric and oligomeric forms of HN. Relevant samples from the same sucrose gradient analysis as shown in Fig. 1 *A* were chosen for immunoprecipitation with the polyclonal HN antibody or the mAbs HN-1b or HN-4b. Three time points after the labeling period were chosen for analysis (15, 30, and 60 min) and only the relevant alternate fractions are shown. Fractions 6–8 contain the oligomerized form of HN and fractions 12–16 contain the monomeric HN.

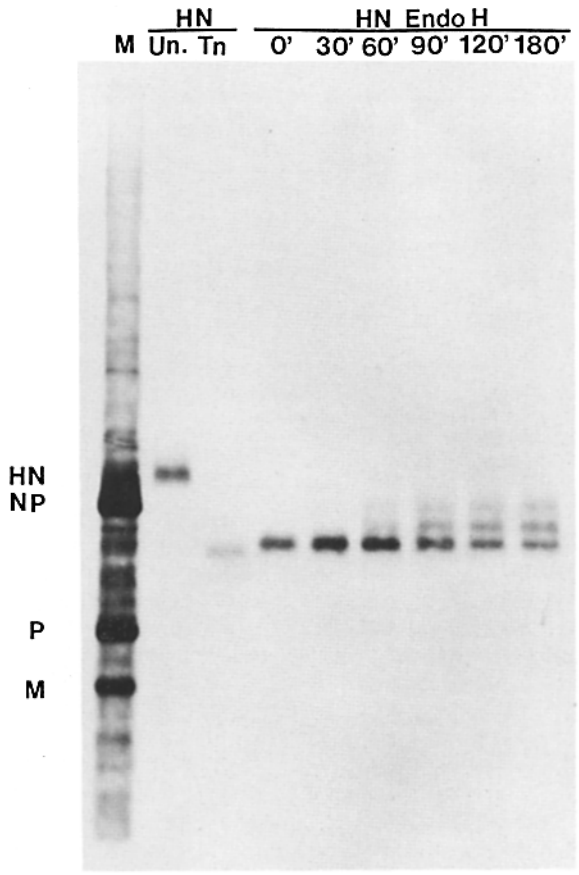

Figure 4. Time course of HN susceptibility to digestion with endoglycosidase H. SV5-infected CV1 cells at 16 h p.i. were labeled with Tran[^{35}S]-label for 15 min. The cells were then incubated for the times indicated in chase medium and lysed in 1% SDS. The lysates were then immunoprecipitated with the polyclonal HN antibody, digested with Endo H and analyzed by SDS-PAGE. Lane *M*, SV5-infected cell marker polypeptides as in Fig. 4; lane *Tn*, unglycosylated HN marker (HN immunoprecipitated from infected cells treated with tunicamycin).

bonds appears to coincide with oligomerization, it is likely that HN-1b binds to an epitope that forms before oligomerization, whereas HN-4b recognizes an epitope that is formed only after oligomerization. To test this possibility, the mAbs were used to immunoprecipitate HN after a 5-min pulse followed by chase periods of 15, 30, and 60 min and fractionation on sucrose density gradients. Only those fractions containing HN polypeptide forms (fractions 6–16, see Fig. 1) were analyzed by immunoprecipitation using the polyclonal HN antibody, antibody HN-1b, or antibody HN-4b. As shown in Fig. 3, after a 15-min chase period most of HN sediments in the slower monomeric peak (fractions 12–16). The mAb HN-1b was reactive with a fraction of HN found in these fractions, whereas HN-4b showed no detectable reactivity with these fractions (cf. lane 16 at 15 min). After 30 and 60 min of chase period, both mAbs were fully reactive to HN found in the faster sedimenting tetrameric peak (fractions 6–8), but again only HN-1b showed any reactivity with the material at the top of the gradient. Thus, these data indicate that the two mAbs have different conformational specificities: HN-1b recognizes a folded form of HN that forms before but is also present after oligomerization and HN-4b is specific to the oligomeric form.

Rate of Transport of HN to the Medial Golgi Complex

N-linked carbohydrate chains are modified from simple to complex carbohydate forms in the Golgi complex, and the presence of carbohydrate chains resistant to digestion with endo-β-N acetylglucosaminidase H (Endo H) is indicative of transport of the glycoprotein through the medial Golgi apparatus (reviewed in reference 26). To determine the rate of transport of HN to the medial Golgi, SV5-infected cells were labeled for 15 min with Tran[^{35}S]-label, incubated for various chase periods, the lysates were immunoprecipitated with the polyclonal HN antibody and immune complexes were digested with Endo H. As shown in Fig. 4, Endo H resistant forms of HN were not detected until 60 min of chase period. Untreated HN and unglycosylated HN synthesized in the presence of tunicamycin were used as markers. Two Endo H-resistant bands with decreased electrophoretic mobility were observed in comparison to the 0-min time point. HN contains four N-linked carbohydrate chains and it has been found that the two Endo H-resistant species represent polypeptides containing either one or two carbohydrate chains of the complex type respectively (Ng D. T. W., S. W. Hiebert, and R. A. Lamb, manuscript in preparation). After longer chase periods, the amount of Endo H resistant forms increased but they did not become a single form, indicating heterogeneity at the same site of *N*-linked sugar addition with different molecules having different carbohydrate modifications i.e., simple or complex. Although not typical, this type of observation has been made previously, e.g., Thy-1 (55). In addition, a population of HN molecules did not acquire Endo H resistance, but in experiments in which antibody was bound to infected cell surfaces, it was found that this unmodified species does become transported to the cell surface (data not shown) and it does not represent a form of oligomerized HN blocked in transport in the Golgi complex. The presence of the multiple species on Endo H treatment made it difficult to measure the precise rate of transport to the medial Golgi complex. However, for purposes of comparison to other proteins, these data indicate that the rate is relatively slow, because for those molecules that become Endo H resistant, <50% of the molecules become Endo H resistant in 60 min.

Subcellular Localization of HN Oligomerization

Oligomerization of HA and G occurs rapidly ($t_{½}$ 7–10 and 6–8 min, respectively) and it has been shown to occur in the ER (6–8, 14). In comparison, HN has a relatively slow rate of oligomerization ($t_{½}$ 25–30 min). As the correct folding and oligomerization of integral membrane proteins have been suggested to be prerequisites for the transport of proteins out of the ER (14, 28), it was of interest to determine the subcellular site of HN oligomerization. To test whether oligomerization of HN occurs before or after transport through this compartment, HN was immunoprecipitated from alternate sucrose gradient fractions (fractions 6–16) after a 5-min pulse-label and varying chase periods, and HN in the immune complexes was digested with Endo H. As shown in Fig. 5, after 5- and 15-min chase periods, when most of HN sedimented at the monomeric position, HN was

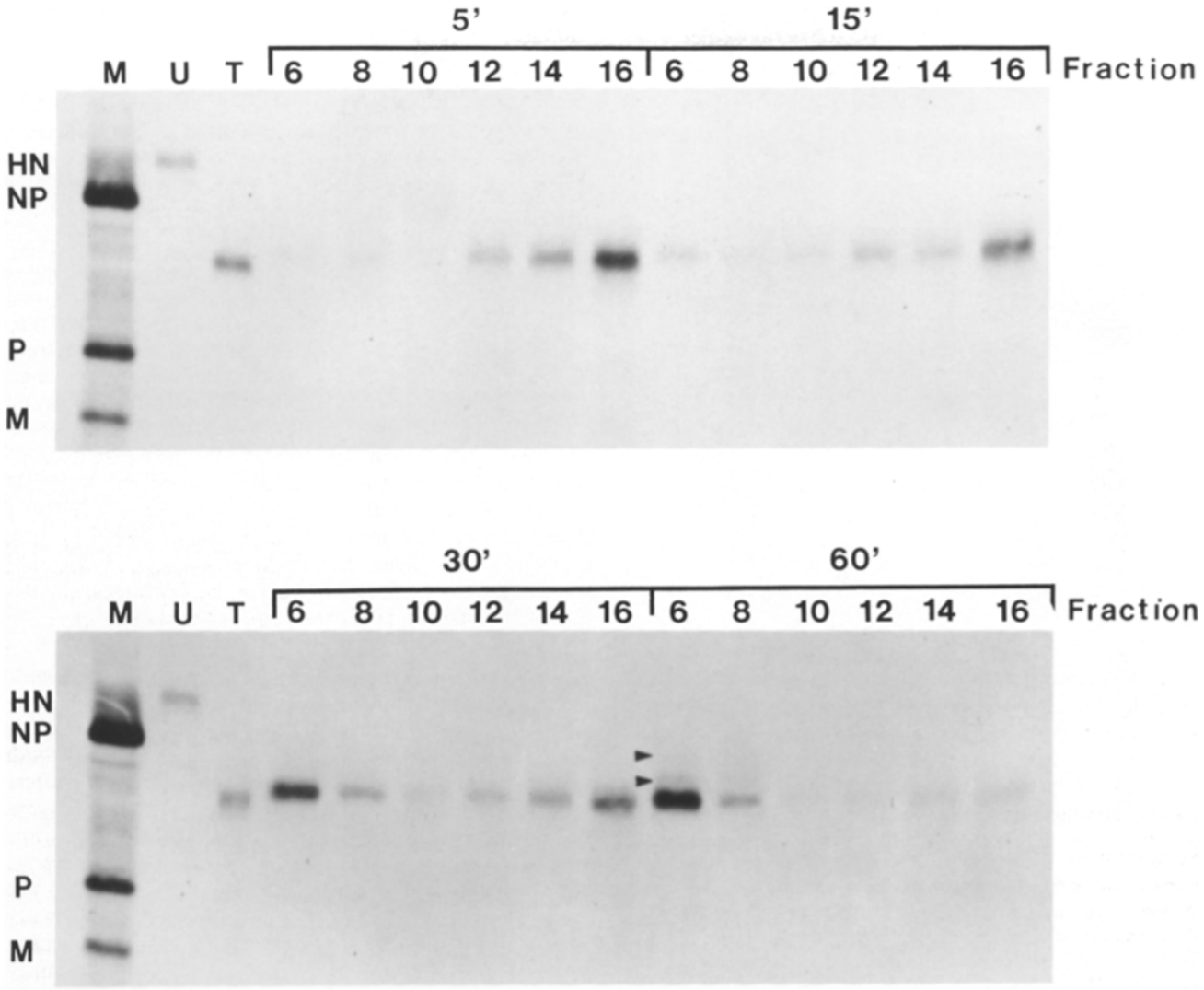

Figure 5. Oligomerization of HN occurs prior to transport to the medial Golgi complex. SV5-infected CV1 cells at 16 h p.i. were pulse-labeled for 5 min with Tran[^{35}S]-label and chased for 0–60 min. At the times indicated, lysates were prepared and fractionated on sucrose velocity gradients. Aliquots from alternate fractions of the relevant region of the gradient were immunoprecipitated with the polyclonal HN antibody and subjected to digestion with Endo H as described in Materials and Methods. *M*, direct lysate of SV5-infected cells as molecular weight markers: *HN*, 66,000; *NP*, 61,000; *P*, 44,000; and *M*, 38,000. *U*, control immunoprecipitated HN marker; *T*, HN synthesized in the presence of tunicamycin as an unglycosylated HN marker. Fraction numbers from each gradient (6–16) are indicated.

entirely Endo H sensitive. After 30 min of chase period, when approximately half of the molecules had assembled into tetramers, HN still remained Endo H sensitive. Only after 60 min of chase period could Endo H-resistant forms of HN be found in the tetrameric position on the gradient (Fig. 5, *arrowheads*). Thus, these data suggest that only oligomeric forms of HN are transported to the medial Golgi apparatus. The rate of oligomerization ($t_{½}$ 25–30 min) and the rate of acquisition of Endo H resistance ($t_{½}$ >60 min) suggests that oligomerization occurs before transport through the medial Golgi complex.

Transport between the ER and the Golgi complex is an energy-dependent process that requires ongoing ATP production (64). CCCP, an uncoupler of oxidative phosphorylation, has been used to block the transport of proteins from the ER (13) and hence its use makes it possible to study the oligomeric form of a protein in the ER (6). To examine further the intracellular site of oligomerization, SV5-infected cells were pulse-labeled for 10 min with Tran[^{35}S]-label and incubated in the absence or presence of CCCP for 2 h in chase medium and then immunoprecipitated with the polyclonal HN antibody or with the oligomer-specific HN-4b. Half of each immune complex was digested with Endo H before samples were analyzed by SDS-PAGE. As shown in Fig. 6, HN was reactive with the HN-4b monoclonal antibody in the presence of CCCP (+). The block in transport to the medial Golgi complex from the ER in the presence of CCCP (+) was confirmed by finding that HN remained sensitive to Endo H digestion, whereas in the absence of CCCP (−), HN acquired Endo H resistance. The recovery of HN precipitated with the HN-4b mAb after CCCP treatment was not as great as with the polyclonal HN antibody, which suggests that a small fraction of molecules was unable to oligomerize in the presence of the drug and some monomeric HN was

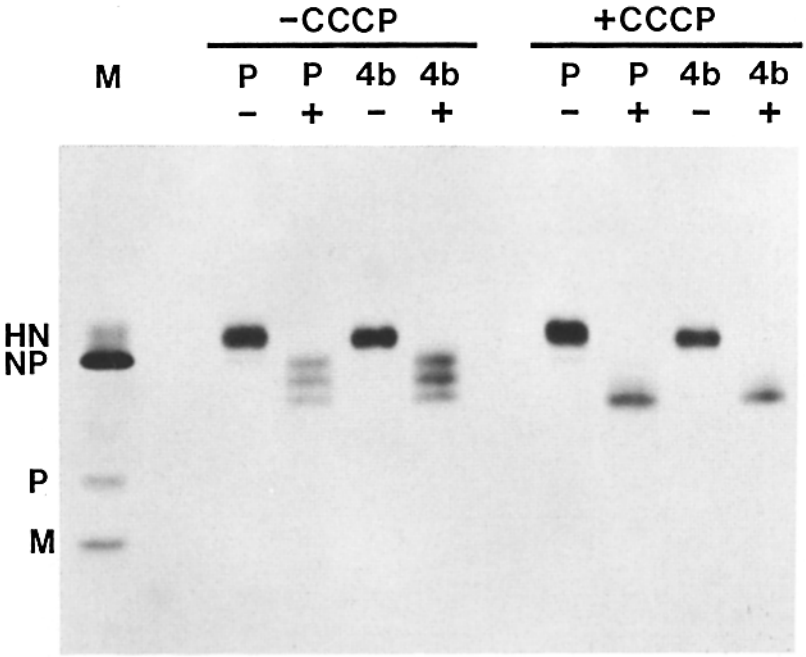

Figure 6. The transport inhibitor CCCP does not block oligomerization. SV5-infected CV1 cells at 14 h p.i. were pulse-labeled for 10 min with Tran[^{35}S]-label. The cells were then incubated at 4°C with prechilled chase medium with (+) or without (−) CCCP (50 μg/ml) for 10 min and then the cultures were shifted to 37°C for 2 h. The cells were then lysed in RIPA buffer and aliquots immunoprecipitated with either the polyclonal HN antibody or mAb HN-4b. Immune complexes bound to protein A-containing agarose beads were either untreated (−) or digested (+) with Endo H. *M*, SV5 marker polypeptides as in Fig. 5; *P*, polyclonal HN antibody; *4b*, mAb HN-4b.

found on sucrose gradient analysis (data not shown). This may indicate a requirement for ATP in folding and oligomerization as has been suggested previously for VSV G (7). Thus, although these data do not prove, they strongly suggest that oligomerization of HN occurs in the ER before its transport to the Golgi complex.

The Specific and Transient Association of GRP78-BiP with HN before Oligomerization

We were interested to determine if the resident ER protein GRP78-BiP has a role in the maturation of the HN protein. In particular, we wished to define whether GRP78-BiP had a specific and transient interaction with HN or if GRP78-BiP only associated with malfolded proteins.

To radioactively prelabel as many as possible of the slowly turning over GRP78-BiP molecules, CV1 cells were labeled with [^{35}S]methionine under steady-state conditions for 24 h. The cells were then infected with SV5 and steady-state [^{35}S]methionine labeling conditions were continued for 16 h p.i. to label all the HN molecules to a similar extent. Samples were then immunoprecipitated with either the polyclonal HN antibody or the mAbs HN-1b or HN-4b. As shown in Fig. 7, lane *4*, in addition to HN, the polyclonal antisera coprecipitated a prominent band that comigrates with GRP78-BiP. The polyclonal HN antibody did not precipitate GRP78-BiP from uninfected cells in which the synthesis of GRP78-BiP had been induced by tunicamycin treatment (Fig. 7, lane *1*), suggesting that coprecipitation of GRP78-BiP and HN is specific. The mAbs HN-1b and HN-4b immunoprecipitated HN in amounts similar to that precipitated by the polyclonal HN antibody but no coprecipitation of GRP78-BiP was observed even after long exposures of the autoradiographs (Fig. 7, lanes *5* and *6*). This indicates that folded forms of HN, as defined by the mAb reactivities, were not associated with GRP78-BiP. To understand further the nature of the population of HN molecules that were associated with GRP78-BiP, sequential rounds of immunoprecipitations were performed. The lysate supernatants from the HN-1b and HN-4b immunoprecipitations were reprecipitated twice with the appropriate monoclonal antibody to assure complete removal of the reactive antigen (Fig. 7, lanes *9* and *10* [HN-1b]; lanes *11* and *12*, [HN-4b]) and then immunoprecipitated with the polyclonal HN antibody, to recover immature and unfolded HN molecules not recognized by the mAbs. As shown in Fig. 7, lanes *7* and *8*, a subpopulation of HN molecules was precipitated by the polyclonal HN sera and it coprecipitated GRP78-BiP in an amount similar to that observed when the polyclonal HN antibody was used on nonadsorbed lysates. These data suggest that this population of HN molecules recovered after preadsorption with the conformation-specific HN-1b or HN-4b mAbs is in a complex with GRP78-BiP. As the mAb reactivity is gained with time after synthesis of HN, the molecules associated with GRP78-BiP are thought to be unfolded and immaturely folded forms of HN. It can be observed in Fig. 7, lanes *7* and *8* that the subpopulation of HN molecules that coprecipitate with GRP78-BiP have a slightly slower electrophoretic mobility than the folded, nonassociated form. This probably represents differences in carbohydrate trimming between the immature and mature forms of HN and further illustrates the authenticity of the two populations of molecules. The polypeptide species seen in lanes *4*, *5*, and *8* of M_r ~34,000 and ~27,000, and indicated by the arrows are proteolytic fragments of HN and they are discussed further below. The other readily identifiable band (M_r ~44,000) is the SV5 P polypeptide, a small amount of which is precipitable by the polyclonal HN antiserum. Preadsorption of the lysate with an anti-P mAb (56) eliminates this band from the gel and does not affect the coprecipitation of HN and GRP78-BiP (data not shown).

The amount of radioactivity in Fig. 7, lanes *6* and *7* was quantitated by densitometry of the autoradiograph and normalized with the known number of methionine residues in both HN and GRP78-BiP (24, 66, 67). A GRP78-BiP to HN ratio >0.7:1 was obtained. As the cells were only steady-state labeled for 40 h and the half-life of GRP78-BiP is >48 h (21), not all molecules of GRP78-BiP present in the ER may be

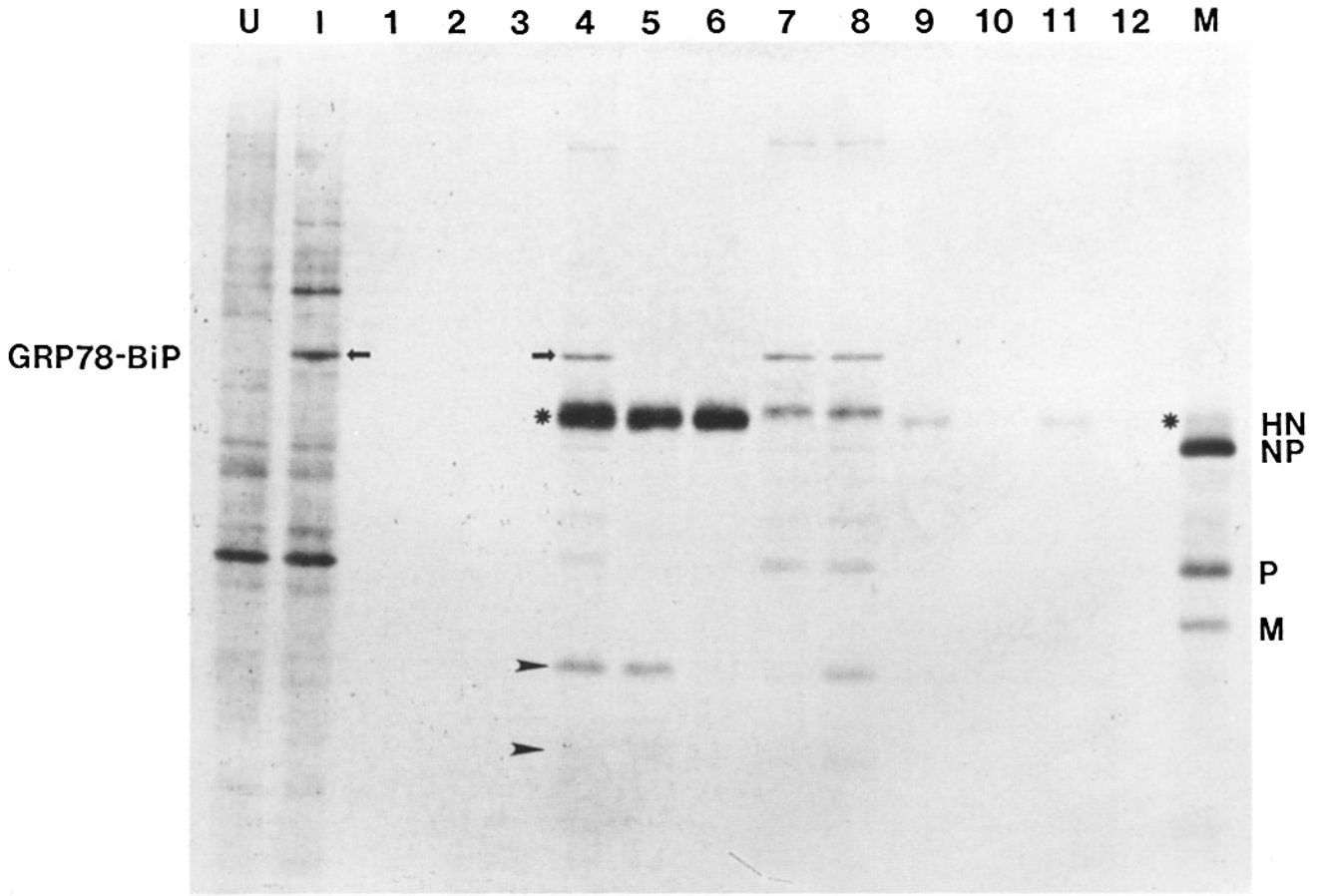

Figure 7. HN associates with the cellular protein GRP78-BiP. CV1 cells were steady-state labeled with [^{35}S]methionine for 24 h as described in Materials and Methods. The cells were then infected with SV5 and steady-state labeling continued for a further 16 h. The cells were then lysed in Triton X-100 under ATP-depleting conditions and aliquots were immunoprecipitated with either the polyclonal HN antibody (lane *4*), mAbs HN-1b (lane *5*) or HN-4b (lane *6*). Lysates absorbed with the mAbs were sequentially immunoprecipitated a second and third time with the same respective antibodies (HN-1b, lanes *9* and *10*; HN-4b, lanes *11* and *12*) to completely deplete the lysate of all HN molecules that were reactive with the mAbs. In the final serial immunoprecipitation, the preabsorbed lysates were incubated with the polyclonal HN antibody to immunoprecipitate HN species not reactive with the mAbs. Lane *7*, lysate depleted of antibody HN-1b reactive forms of HN; lane *8*, lysate depleted of antibody HN-4b reactive forms of HN. Control immunoprecipitations of steady-state labeled mock-infected CV1 cells treated with tunicamycin (1 μg/ml) (to induce high-expression levels of GRP78-BiP) were done with polyclonal HN antibody (lane *1*), antibody HN-1b (lane *2*), and antibody HN-4b (lane *3*). Lane *U*, direct lysate of uninduced steady-state labeled cells; lane *I*, direct lysate of tunicamycin treated steady-state labeled cells. The arrow indicates GRP78-BiP, the asterisk indicates HN and arrowheads mark the positions of the M_r ~34,000 and ~27,000 degradation products of HN that are recognized by antibodies HN-1b and the polyclonal HN antibody but not antibody HN-4b; these species are discussed further below with respect to data shown in Fig. 9.

labeled. Thus, the finding of a ratio of GRP78-BiP to HN of 0.7:1 suggests that HN may form a complex with one (or more) molecules of GRP78-BiP.

To investigate whether GRP78-BiP transiently associated with HN as a normal event during the maturation of HN or if GRP78-BiP was only binding to malfolded HN molecules that were not recognized by the mAbs, the kinetics of association of GRP78-BiP with HN were examined with respect to HN folding. SV5-infected CV1 cells were pulse-labeled for 5 min with Tran[^{35}S]-label and incubated in chase medium for varying periods before lysis of the cells in ATP-depleting detergent buffer. Serial immunoprecipitations were performed with the rat anti-BiP mAb (kindly provided by Drs. Linda Hendershot and John Kearney), the mAb HN-1b, and lastly anti-HN IgG. Based on the experiment described in Fig. 7, it was predicted that if GRP78-BiP had a specific but transient association with HN, the BiP antibody would coprecipitate HN in a time-dependent manner and before the conformation-specific monoclonal HN-1b would recognize HN. Immunoprecipitation with the polyclonal HN antibody was done in the third round of precipitations to recover all forms of HN not removed by the first two antibodies so that it was possible to account for all the labeled HN synthesized, especially as the association of GRP78-BiP with HN is labile and multiple rounds of immunoprecipitation may dissociate some HN from GRP78-BiP.

The results of this time-course experiment (Fig. 8) show that immediately after a 5-min pulse-label, the BiP antibody precipitates a large part of the labeled HN and thus it is in a complex with GRP78-BiP. With longer chase periods, HN loses its association with GRP78-BiP and is no longer coprecipitated by the BiP antibody (Fig. 8 *A*). Concomitantly, HN gains its ability to react with the conformation-specific monoclonal antibody (Fig. 8 *B*) and this is at the same rate as ob-

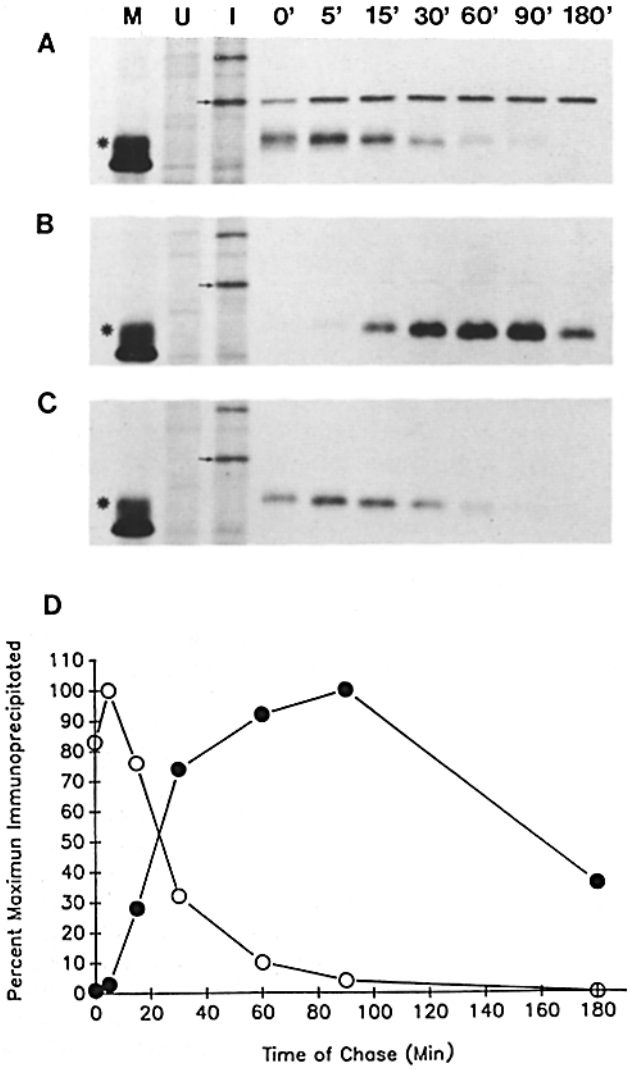

Figure 8. Association of HN and GRP78-BiP is specific and transient and occurs prior to complete folding and oligomerization. SV5-infected CV1 cells at 16 h p.i. were pulse-labeled for 5 min with Tran[^{35}S]-label. The cells were then incubated in chase medium for the times indicated and lysed in Triton X-100 under ATP-depleting conditions. Nuclei and debris were removed by centrifugation and the supernatants were serially immunoprecipitated with anti-BiP monoclonal antibody (*A*), followed by mAb HN-1b (*B*), and finally the polyclonal HN antibody (*C*). Lane *M*, SV5 protein markers (HN indicated by an asterisk); lane *U*, uninduced cell lysate; lane *I*, tunicamycin treated cell lysate. GRP78-BiP is indicated by an arrow. (*D*) quantitation by laser-scanning densitometry of HN in autoradiographs from *A* and *B*. *Open circle*, HN associated with GRP78-BiP; *filled circle*, HN reactive with antibody HN-1b.

served without prior precipitation with the BiP antibody (see Fig. 2). The data shown in Fig. 8, *A* and *B* were quantitated by densitometric scanning and are shown in Fig. 8 *D* to show the inverse relationship between BiP antibody binding HN and the HN-1b antibody binding. Preadsorption of the lysates with anti-BiP did not affect the results obtained with HN-1b as it was shown in Fig. 7 that HN-1b was not reactive against GRP78-BiP associated forms of HN. The small amount of GRP78-BiP that can be seen on the autoradiograph (Fig. 8 *B*) is due to carrying over some anti-BiP/GRP78-BiP immune complexes in the procedure and it does not affect the result. The polyclonal HN antibody precipitated immature HN molecules (Fig. 8 *C*) that were either not complexed or had dissociated from GRP78-BiP, during the procedure.

Of critical importance to the interpretation of these data is the quantitation of all the labeled HN molecules synthesized. It could initially be thought that the HN molecules shown in Fig. 8 *A* only represent malfolded HN molecules bound to BiP that are rapidly degraded in the ER and that only the immature HN molecules recognized by the polyclonal antisera (*C*) give rise to the mature species of HN recognized by the HN-1b antibody (*B*). At 5 min chase, the HN molecules shown in *A* are ~60% of the total HN molecules present in *B* at 90 min chase, and the HN molecules in *C* at 5 min chase are ~40% of the HN molecules shown in *B* at 90 min chase (there is little degradation of HN until 60–90 min, when measured using a 5-min pulse-label). Therefore, although the molecules shown in *C* are maturing into the folded form shown in *B*, HN molecules originally associated with BiP (*A*) have to be maturing and contributing greatly to the population of HN molecules found in *B* and thus these data are inconsistent with these HN molecules being rapidly degraded in the ER. Indeed, artificially engineered malfolded HN molecules form a stable association with BiP that turns over slowly ($t_{½}$ ~6 h) (Ng D. T. W., S. Hiebert, and R. A. Lamb, manuscript in preparation). Given the observation that it is difficult to coprecipitate all of the cellular GRP78-BiP protein complexes with the BiP antibody (21) and the caveat discussed above concerning dissociation of BiP-complexes during repeated precipitations, these data indicate that a large proportion, if not all, of HN associates with GRP78-BiP during, or shortly after, synthesis and dissociates from GRP78-BiP when it attains a folded conformation. Thus, it seems reasonable to suggest that the GRP78-BiP and HN interaction is specific and part of the normal maturation pathway of HN.

Other polypeptide species were also observed to be coprecipitated by the BiP antibody and these are presumed to be cellular polypeptides localized in the ER. However, in comparison to HN they were found in very low abundance (data not shown). A specific association between GRP78-BiP and the SV5 F glycoprotein has not been observed. However, this does not rule out the possibility that this interaction exists, as the conditions used may not be suitable for detecting a transient association with F, as our preliminary results indicate that the maturation of F is more rapid than HN (data not shown).

HN is Rapidly Turned Over in Cells

In experiments in which SV5-infected CV1 cells were pulse-labeled and incubated for varying chase periods, it was observed that the amount of HN precipitated declined with time (e.g. see Fig. 8 *D*). To investigate this further, infected cells were labeled for 15 min with Tran[^{35}S]-label, incubated for up to 7 h in chase medium and HN immunoprecipitated with the polyclonal HN antibody. As shown in Fig. 9 *A*, HN is turned over with a $t_{½}$ of 2–2.5 h. It seemed possible that the loss of HN would be attributable to shedding from cell surfaces or to its incorporation into budding and released virus particles. However, this was not the case, as <1% of the total HN present at 0 time could be recovered from the medium after 7 h (data not shown). Longer exposures of the autora-

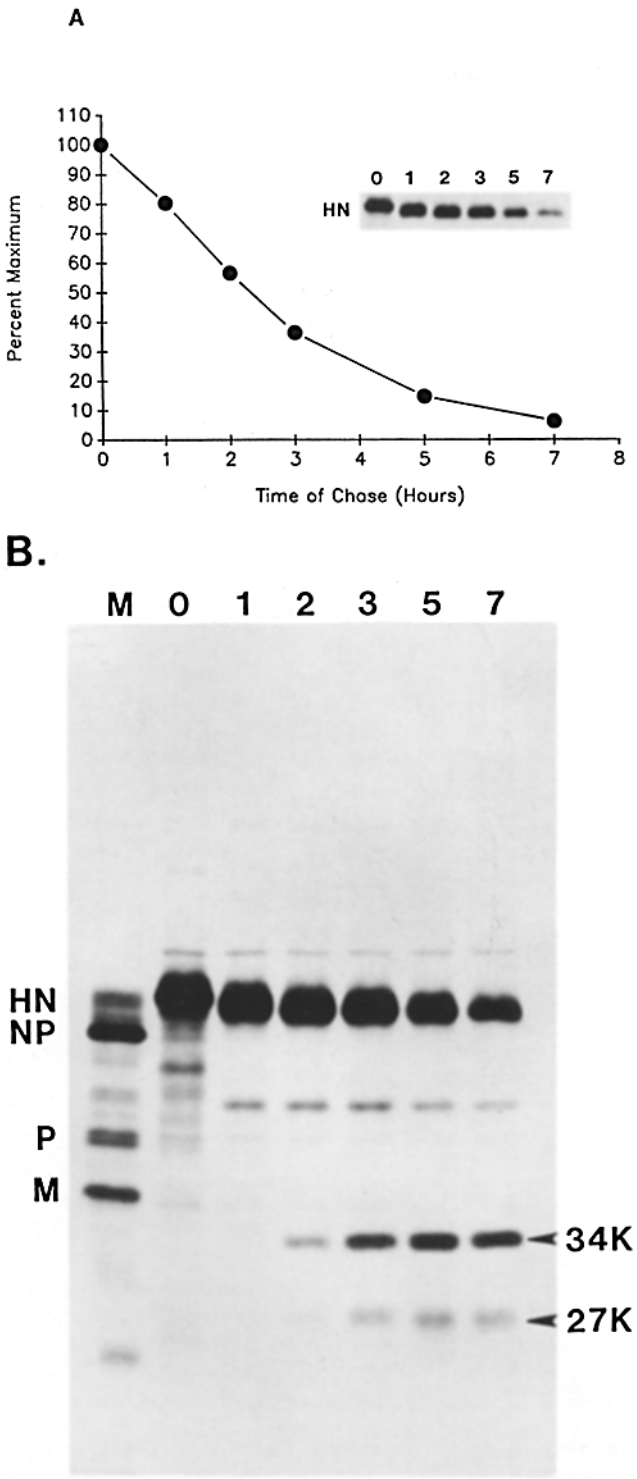

Figure 9. HN does not accumulate in infected cells and is turned-over. SV5-infected CV1 cells at 14 h p.i. were labeled for 15 min with Tran[^{35}S]-label and incubated in chase medium for varying periods from 0–7 h. The cells were lysed in RIPA buffer and HN immunoprecipitated with the polyclonal HN antibody. Polypeptides were analyzed by SDS-PAGE. (*A*) autoradiograms like that shown in the insert, were quantitated by laser scanning densitometry and the average values from three experiments are plotted showing the percent maximum HN immunoprecipitated with time of chase in hours. (*B*) over exposure of time-course of stability of HN to show the HN cleavage products of M_r ~34,000 and ~27,000, which are indicated by the arrowheads. The time of chase is indicated above each lane in hours. *M*, SV5 marker polypeptides as in Fig. 5.

diograms from these experiments (Fig. 9 *B*) indicated the presence of two HN species (M_r ~34,000 and ~27,000) of which the amount recovered does not reflect the amount of HN lost. It seemed likely that the loss of HN is by a degradative process and that these species are intermediates in the degradation of HN. It is interesting to note that these smaller HN specific species could be immunoprecipitated by the HN-1b but not the HN-4b mAb (see Fig. 7, lanes *5* and *6*), suggesting preservation of specific domains after cleavage. In parallel experiments, F, the other glycoprotein of SV5, was found to be relatively stable (data not shown).

HN Is Extensively Internalized from the Cell Surface

It has long been known that HN is expressed at the surface of SV5-infected cells and is incorporated into virus particles (see reference 4). However, the rapid turnover of HN made it difficult to determine its rate of arrival at the cell surface. We investigated the possibility that HN was internalized from the cell surface and transported to internal cellular compartments, possibly lysosomes, for degradation. To test this hypothesis, either mAb HN-1b or F-1a was bound to the surface of SV5-infected cells and incubated at 4°C, a temperature that blocks internalization (63). Unbound antibody was removed by washing the monolayers and the cells were then incubated in prewarmed media at 37°C in the presence or absence of 100 μM chloroquine. At various times after the temperature shift, cells were processed for intracellular fluorescence. The bound HN- or F-specific antibody was detected by staining with FITC-conjugated goat anti-mouse IgG. As shown in Fig. 10, antibody bound to HN at the cell surface was internalized and localized in scattered intracellular vesicles after 30 min (cf. *A* and *D*). After 60 min, the fluorescent vesicles were less dispersed and began to aggregate near the nuclei of cells (*G*) and by 120 min the staining pattern was perinuclear (*J*) and virtually identical to the intracellular staining pattern obtained when HN-1b antibody was bound directly to permeabilized cells (cf. Fig. 10 *J* to Fig. 11 *B*). Mock-infected cells treated in parallel did not exhibit a similar staining pattern (Fig. 10, *C*, *F*, *I*, and *L*). Treatment of SV5-infected cells with the lysosomotropic agent chloroquine did not block internalization of antibody-bound HN. However, the stained vesicles became enlarged and remained dispersed 120 min after the temperature shift (Fig. 10, *B*, *E*, *H*, and *K*) as would be expected if antibody-bound HN was localized to intracellular vesicles that were blocked in transport to lysosomes due to the chloroquine treatment (38). Cell surface fluorescent staining of HN-1b antibody bound to HN provided further support for internalization. After binding of HN-1b to cell surfaces but before the temperature shift, the cell surface staining pattern was punctate (Fig. 10 *M*). After 120 min of incubation at 37°C cell surface staining was not observed (Fig. 10 *P*), which is consistent with internalization of the antibody. In contrast to the situation with HN, when the same experiment was performed using F-1a antibody bound to the cell surface, the staining pattern before and 120 min after the temperature shift was similar (Fig. 10, *N* and *Q*). In addition the intracellular staining pattern of F-1a antibody, before and 120 min after the temperature shift did not differ significantly, although some faintly staining vesicles could be observed (Fig. 10, *O* and *R*).

Although the above data indicate that HN is internalized from the cell surface when bound to antibody, whereas in the

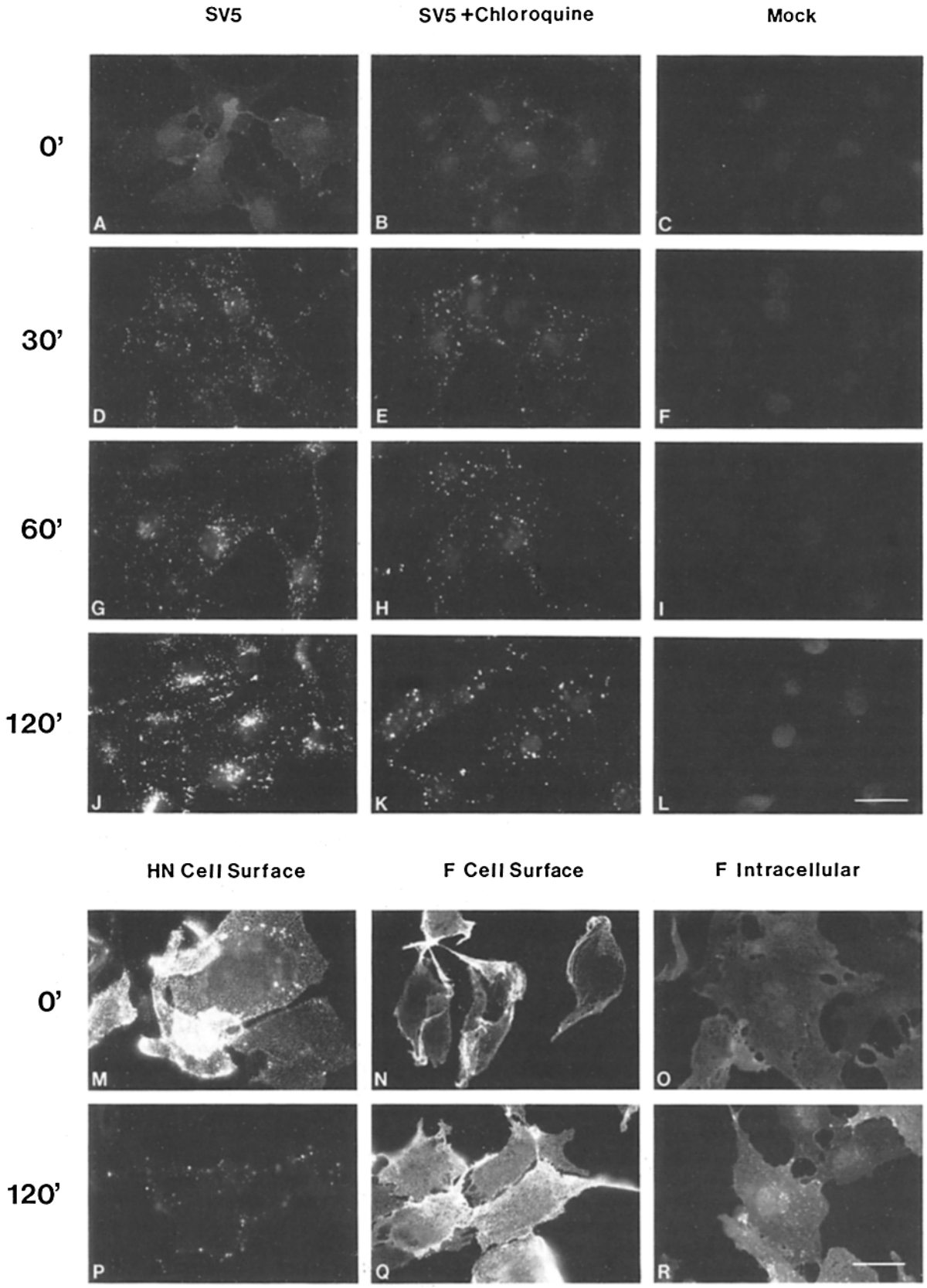

Figure 10. HN-antibody complexes are rapidly internalized from the cell surface: F-antibody complexes are stable. Coverslips of SV5-infected CV1 cells at 14 h p.i. were washed with prechilled PBS and incubated at 4°C to prevent glycoprotein transport and internalization of surface molecules. mAbs specific to HN (HN-1b) or to F (F-1a) were added to the cells at 4°C and allowed to bind surface antigen for 30 min and then the cells were extensively washed in PBS at 4°C. The medium was replaced with prewarmed DME and the cells incubated at 37°C for varying periods. Cells were fixed with formaldehyde for surface staining or fixed with formaldehyde and permeabilized with

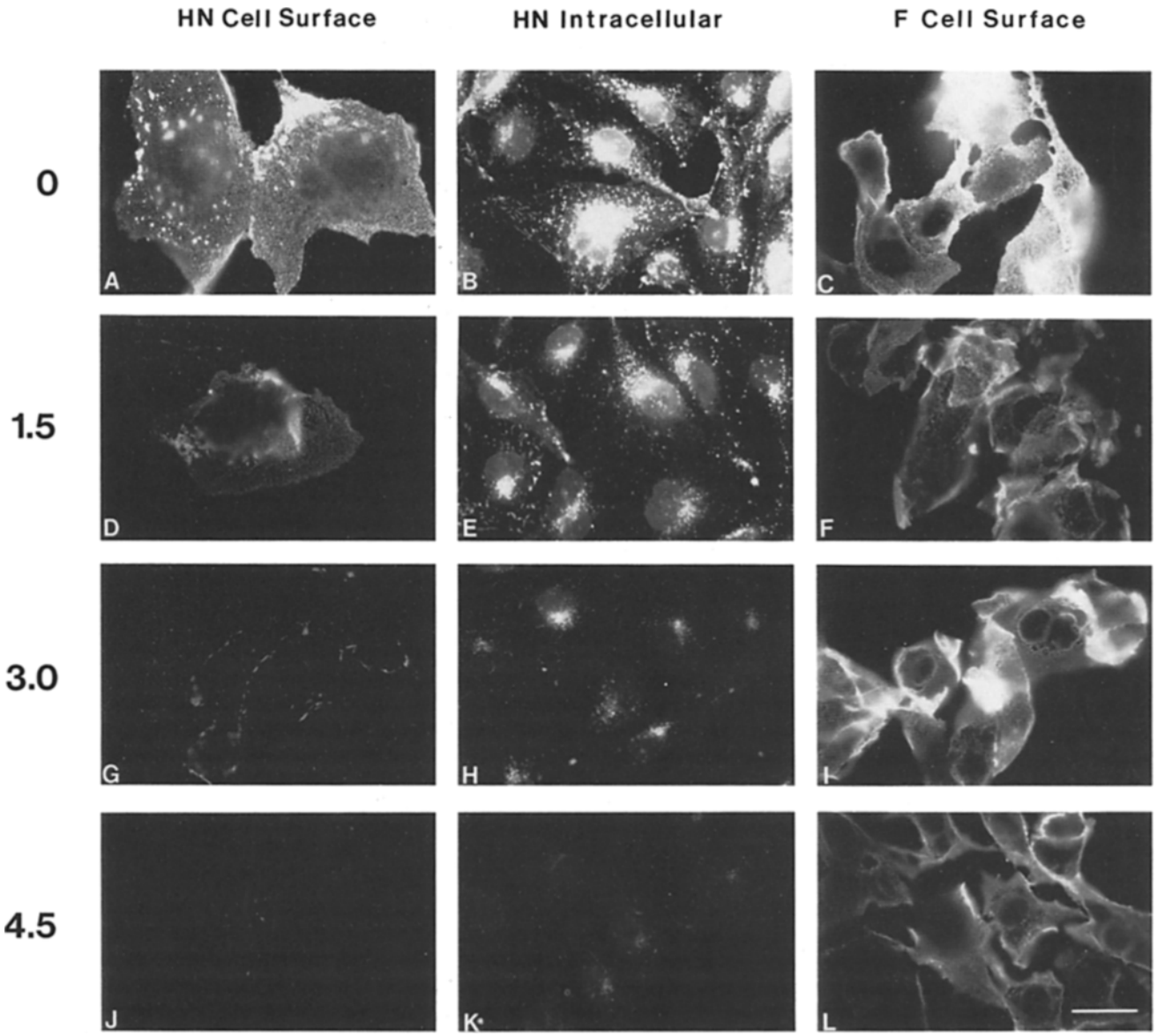

Figure II. HN internalization is not antibody mediated. SV5-infected cells at 16 h p.i. were incubated with 100 μg/ml cycloheximide to inhibit further protein synthesis. At various times cells were fixed, or fixed and permeabilized, for indirect immunofluorescent staining of HN or F as described in Materials and Methods. The panels show HN cell surface staining (*A*, *D*, *G*, and *J*) and HN intracellular staining (*B*, *E*, *H*, and *K*) at 0, 1.5, 3, and 4.5 h respectively after the beginning of the cycloheximide treatment. Parallel infected cell cultures were stained for F at the cell surface (*C*, *F*, *I*, and *L*) at the same indicated times. Micrographs in each series were both photographed and printed with identical times of exposure. Bar, 10 μm.

large part F is not, it does not exclude the possibility that the binding of antibody has an effect on this process. If HN follows a degradative pathway rather than a recycling pathway and this process is antibody independent, then it should be possible to monitor the loss of HN from cell surfaces and from intracellular vesicles when protein synthesis is inhibited. To test this hypothesis, SV5-infected cells at 16 h p.i. were treated with the inhibitor of protein synthesis cycloheximide (100 μg/ml) which in CV1 cells is 98% efficient at inhibiting protein synthesis (data not shown). At various times,

acetone for intracellular staining. HN- and F-bound antibodies were stained by the addition of fluorescein-conjugated goat anti-mouse antibody. The intracellular staining pattern of antibody-HN complexes internalized from infected cell surfaces from 0 to 120 min following the temperature shift are shown in *A*, *D*, *G*, and *J*. Infected cells treated with chloroquine are shown in *B*, *E*, *H*, and *K*, and mock-infected cells in *C*, *F*, *I*, and *L* and the times after the temperature shift are indicated. (*M* and *P*) Cell surface staining of HN before and 2 h after the temperature shift, respectively. (*N* and *Q*) Cell surface staining of F before and 2 h after temperature shift, respectively. (*O* and *R*) Intracellular staining of F before and 2 h after the temperature shift, respectively. Micrographs in each series were both photographed and printed with identical exposure times. Bar, 10 μm.

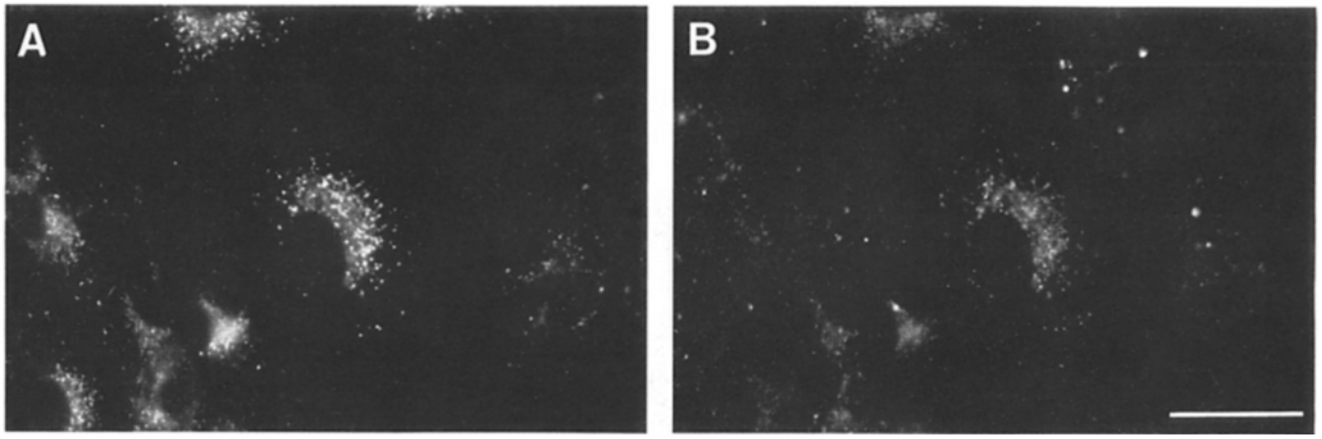

Figure 12. HN colocalizes with a marker for lysosomes. SV5-infected CV1 cells at 16 h p.i. were incubated for 2 h in DME containing 100 μg/ml of Texas Red (TR)-conjugated ovalbumin. The cells were then fixed and permeabilized and stained for HN using monoclonal antibody HN-1b and fluorescein-conjugated goat anti-mouse antibody. (*A*) Fluorescein staining of HN. (*B*) Texas red staining of ovalbumin in the same field of cells as *A*. Bar, 10 μm.

monolayers were fixed, or fixed and permeabilized, for indirect immunofluorescence. The cells were then incubated with mAb HN-1b or F-1a and stained with FITC-conjugated goat anti-mouse antibody. As shown in Fig. 11, HN staining was lost from the surface of cells with time, and was barely detectable 3 h after the cessation of protein synthesis (Fig. 11, *A*, *D*, *G*, and *J*). The intracellular HN staining pattern also decreased over this period, suggesting that HN was being degraded (Fig. 11, *B*, *E*, *H*, and *K*). The perinuclear HN staining pattern in this experiment was very similar to that observed when HN-antibody complexes were internalized. As expected, the cell surface staining pattern for the F glycoprotein was relatively unchanged over the 4.5-h period of treatment with cycloheximide (Fig. 11, *C*, *F*, *I*, and *L*). Together, the data in Figs. 10 and 11 indicate that HN transported to the cell surface in SV5-infected cells is sorted for internalization away from the F glycoprotein.

HN Colocalizes with a Marker for Lysosomes

To further define the sub-cellular localization of HN, double-label immunofluorescence was performed with Texas Red (TR)-conjugated ovalbumin as an endocytic marker that is taken up by cells nonspecifically and accumulates in lysosomes (32). SV5-infected cells were incubated with TR-conjugated ovalbumin (100 μg/ml) for 2 h and then formaldehyde-fixed and permeabilized in acetone. HN was stained by the addition of the mAb HN-1b and FITC-conjugated goat anti-mouse IgG. Fig. 12 shows the fluorescein-labeled HN (*A*) and TR-conjugated ovalbumin (*B*) in the same field of cells. Most of the staining was found to be coincident, suggesting that HN is localized to lysosomes as well as endocytic vesicles.

Discussion

Several models for the intracellular sorting of proteins in the exocytic pathway have been proposed (reviewed in reference 52). Because of the different rates of exit of proteins from the ER after synthesis, it has been argued that transport occurs via a selective mechanism requiring positively acting signals (12, 33). Alternatively, it has been proposed that transport to the cell surface is by default and is mediated by a continuously moving "conveyor belt" of vesicles (bulk flow) from the ER to the cell surface and that sorting would be achieved by the specific retention of proteins in the ER or Golgi apparatus (59, 71). This proposal is based on finding a very fast rate ($t_{½}$ 10–20 min) of transport of a synthetic glycopeptide, which is thought unlikely to contain selective and positively acting transport signals (71). However, these two general schemes do not have to be mutually exclusive as polypeptides could be retained in the ER while they fold and oligomerize, and during this maturation process a positively acting transport signal could be formed that is necessary for exit from the ER.

In our studies on the maturation and assembly of the class II integral membrane protein HN of the paramyxovirus SV5 we found, using sucrose velocity gradient analysis and antibodies specific for different conformational forms of the protein, that oligomerization occurred with a $t_{½}$ of 25–30 min. Oligomerization of the majority of known membrane and secretory proteins is thought to occur in the ER (57). Support for the idea that HN oligomerization takes place in the ER was provided by finding that it occurred in the presence of the transport inhibitor CCCP, and also by the finding that whereas the $t_{½}$ of oligomerization is 25–30 min, the $t_{½}$ for gaining Endo H resistance is >60 min. This implies that HN oligomerizes long before it reaches the medial Golgi. Direct evidence for this was provided by finding that HN oligomers were formed before they acquired Endo H resistance and that HN monomers always remained Endo H sensitive. HN becomes an oligomer slowly as compared with the rates of assembly of the influenza virus HA ($t_{½}$ 7–10 min) (14) or VSV G ($t_{½}$ 6–8 min) (7). Additionally, the rate of arrival of SV5 HN at the medial Golgi complex is relatively slow has also been observed for the HN molecule of the related paramyxoviruses, Newcastle disease virus and Sendai virus ($t_{½}$ 60 min) (41, 42), and this is in contrast to the rapid rates for VSV G and influenza HA ($t_{½}$ 15–20 min) (5, 35). As the rate at which proteins traverse the Golgi complex and arrive at the cell surface is thought to be similar (12, 33), it seems possible that the difference in rates of folding and oligomerization may account in part for the differences in exit time from the ER.

As the folding and oligomerization process of HN is a relatively slow process, we were interested in investigating if the resident ER component GRP78-BiP recognized and interacted with HN during its maturation. We have found that a substantial amount of GRP78-BiP associates with unfolded forms of HN as judged by the reactivity of these species with the polyclonal HN antibody after depletion of all HN species reactive with the mAbs. The form of HN that interacts with GRP78 is monomeric and has not acquired Endo H resistance (data not shown) as would be expected for the unfolded forms of HN. Quantitation of the molar amount of GRP78-BiP (labeled under steady-state conditions) that associates with HN, indicated a ratio >0.7:1. As GRP78-BiP has a half-life of >48 h (21), and thus it is difficult to label all molecules, it seems possible that all unfolded molecules of HN are associated with one (or more) molecules of GRP78-BiP. The kinetic analysis of the HN/GRP78-BiP interaction strongly suggests that this association is specific and transient ($t_{½}$ 20–25 min), as GRP78-BiP was found complexed with HN during or immediately following its synthesis and dissociation occurred when HN began to form its folded conformation. It has been found that ATP dissociates GRP78-BiP complexes in vitro (43). Addition of 1 mM ATP to the HN/GRP78-BiP complexes caused dissociation of the interaction and the unfolded status of the HN molecules was confirmed by finding that these HN species did not react with the HN monoclonal antibodies (data not shown). These findings also argue against the possibility that GRP78-BiP was binding to the epitope recognized by the antibodies.

The specific and transient association of GRP78-BiP with HN during its maturation pathway and the inverse correlation of this association with HN folding and oligomerization suggests that this is a normal role of GRP78-BiP, as was suggested previously for the assembly of immunoglobulins (1, 20). The GRP78-BiP interaction with HN may be important to retain HN in the ER. During the slow process of folding and oligomerization, the resident ER protein disulfide isomerase (2) is likely to be involved in the formation of complex intramolecular and intermolecular disulfide bonds, thus GRP78-BiP may prevent unfolded forms from entering the exocytic pathway. We speculate that the interaction of GRP78-BiP may be mediated by a "transient retention signal" in HN that is exposed during or shortly after translocation of HN into the ER but that is buried on folding of the molecule. Further evidence for a role of GRP78-BiP in the maturation of HN comes from work done with HN molecules lacking *N*-linked glycosylation sites. These altered molecules neither fold properly to gain reactivity with the monoclonal antibodies nor do they oligomerize and they are retained in the ER in a stable complex ($t_{½}$ ~6 h) with GRP78-BiP (Ng et al., manuscript in preparation). The finding that the association of GRP78-BiP with HN is part of its maturation pathway in the ER, supports the proposal that GRP78-BiP may be a member of a recently described group of proteins called chaperonins, which are involved in the posttranslational assembly of multi-subunit proteins (16, 19, 48).

Our studies on the internalization of HN developed from the observation that HN is rapidly turned over in cells and this had made it difficult to determine the rate of transport of HN to the cell surface. Initially it was assumed that turnover would be explained by the shedding of HN molecules from the cell surface or due to the incorporation of HN into budding virus particles but neither of these two possibilities were found to be correct. HN was found to be extensively internalized from the cell surface and became localized in intracellular vesicles and lysosomes. In the absence of synthesis of HN, fluorescent staining of lysosomes was lost with time, and together with the biochemical data for the turnover of HN, these data suggest that endocytosis of HN is of the nonrecycling type and that internalized HN is degraded in lysosomes. However, these data do not exclude the possibility that some of the turnover of HN is attributable to its direct transport from the Golgi apparatus to lysosomes. Although both the SV5 HN and F glycoproteins must be close in proximity to form a patch on the cell surface for virus budding (see reference 4), HN must be sorted away from the F protein at the cell surface as F accumulates there. The HN internalization experiments were performed with SV5-infected CV1 cells and these cells do not produce as many infectious particles as MDBK cells (3, 49). Thus, it might be thought that HN internalization would affect the number of maturing virus particles. However, when the experiments were performed in SV5-infected MDBK cells it was found that HN had as rapid a rate of turnover as in CV1 cells (data not shown). Additionally, we have found that the turnover of HN is not dependent on the expression of other SV5 proteins as it occurs at a similar rate in CV1 cells that express HN from an SV40-HN recombinant vector (data not shown).

Unlike the situation occurring with SV5, in cells infected with Sendai virus, a related paramyxovirus, internalization of HN does not seem to occur (60). However, in cells infected with a mixture of standard and defective Sendai virus particles, in which there is a poor level of accumulation of the viral matrix protein (M) it was found that HN was internalized and it was hypothesized that the mechanisms underlying these observations are interconnected (60). Retrospective analysis of photomicrographs showing fluorescent intracellular staining of the HN protein of the related mumps virus (70) show a vesicular pattern that is very similar to that found with SV5, which suggests that internalization of these viral type II integral membrane proteins may be a frequent occurrence.

The most common pathway for cellular plasma membrane receptors is that they are recycled to the cell surface after endocytosis (reviewed in reference 15). However, endocytosis and degradative processes are used by several cellular receptors e.g., IL-2 receptor (11) and tumor necrosis factor receptor (68): these receptors internalize with and without ligand and are eventually degraded. Although the physiological significance of degradation of HN in tissue culture cell infections with SV5 is presently unclear, in an animal infection it may have great importance in removing the highly immunogenic HN molecule from immune surveillance and causing persistent infection by allowing cell to cell spread of virus by the viral fusion activity. The SV5 HN molecule will also provide a useful model system for studying further aspects of the endocytosis/degradative pathway.

We thank Margaret A. Shaughnessy for excellent technical assistance. We are very grateful to Linda Hendershot and John Kearney for providing the BiP antibody, and Reay G. Paterson, Stephanie S. Watowich, and Mark A. Williams for helpful discussions.

This research was supported by Public Health Service research awards AI-20201 and AI-23173 from the National Institute of Allergy and Infectious Diseases. D. T. W. Ng was supported by a National Institutes of

Health Training Program in Cell and Molecular Biology (GM-08061). R. E. Randall is the recepient of a Wellcome Trust University Award.

Received for publication 28 June 1989 and in revised form 16 August 1989.

References

1. Bole, D. G., L. M. Hendershot, and J. F. Kearney. 1986. Posttranslational association of immunoglobulin heavy chain binding protein with nascent heavy chains in nonsecreting and secreting hybridomas. *J. Cell Biol.* 102:1558–1566.
2. Bulleid, N. J., and R. B. Freedman. 1988. Defective co-translational formation of disulfide bonds in protein disulfide-isomerase-deficient microsomes. *Nature (Lond.).* 335:649–651.
3. Choppin, P. W. 1964. Multiplication of a myxovirus (SV5) with minimal cytoplasmic effects and without interference. *Virology.* 23:224–233.
4. Choppin, P. W., and R. W. Compans. 1975. Reproduction of paramyxoviruses. *In* Comprehensive Virology. Vol. 14. H. Fraenkel-Conrat and R. R. Wagner, editors. Plenum Publishing Corp. New York. 95–178.
5. Copeland, C. S., R. W. Doms, E. M. Bolzau, R. G. Webster, and A. Helenius. 1986. Assembly of hemagglutinin trimers and its role in intracellular transport. *J. Cell Biol.* 103:1179–1191.
6. Copeland, C. S., K.-P. Zimmer, K. R. Wagner, G. A. Healey, I. Mellman, and A. Helenius. 1988. Folding, trimerization, and transport are sequential events in the biogenesis of influenza virus hemagglutinin. *Cell.* 53:197–209.
7. Doms, R. W., D. S. Keller, A. Helenius, and W. E. Balch. 1987. Role of adenosine triphosphate in regulating the assembly and transport of vesicular stomatitis virus G protein trimers. *J. Cell Biol.* 105:1957–1969.
8. Doms, R. W., A. Ruusala, C. Machamer, J. Helenius, A. Helenius, and J. K. Rose. 1988. Differential effects of mutations in three domains on folding, quaternary structure, and intracellular transport of vesicular stomatitis virus G protein. *J. Cell Biol.* 107:89–99.
9. Dorner, A. J., D. G. Bole, and R. J. Kaufman. 1987. The relationship of N-linked glycosylation and heavy chain-binding protein association with the secretion of glycoproteins. *J. Cell Biol.* 105:2665–2674.
10. Drummond, I. A. S., A. S. Lee, E. Rosendez, Jr., and R. A. Steinhardt. 1987. Depletion of intracellular calcium stores by the calcium ionophore A23187 induces the genes for the glucose-regulated proteins in hamster fibroblasts. *J. Biol. Chem.* 262:12801–12805.
11. Duprez, V., and A. Daltry-Versat. 1986. Receptor mediated endocytosis of interleukin 2 in a human tumor T-Cell line. *J. Biol. Chem.* 261: 15450–15454.
12. Fitting, T., and D. Kabat. 1982. Evidence for a glycoprotein "signal" involved in transport between subcellular organelles. *J. Biol. Chem.* 257:14011–14017.
13. Fries, E., and J. E. Rothman. 1980. Transport of vesicular stomatitis virus glycoprotein in a cell-free extract. *Proc. Natl. Acad. Sci. USA.* 77: 3870–3874.
14. Gething, M.-J., K. McCammon, and J. Sambrook. 1986. Expression of wild-type and mutant forms of influenza hemagglutinin: the role of folding in intracellular transport. *Cell.* 46:939–950.
15. Goldstein, J. L., M. S. Brown, R. G. W. Anderson, D. W. Russell, and W. J. Schneider. 1985. Receptor-mediated endocytosis: concepts emerging from the LDL receptor system. *Annu. Rev. Cell Biol.* 1:1–39.
16. Goloubinoff, P., A. A. Gatenby, and G. H. Lorimer. 1989. GroE heatshock proteins promote assembly of foreign prokaryotic ribulose bisphosphate carboxylase oligomers in *Escherichia coli*. *Nature (Lond.).* 337: 44–47.
17. Gottlieb, T. A., A. Gonzalez, L. Rizzolo, M. J. Rindler, M. Adesnik, and D. D. Sabatini. 1986. Sorting and endocytosis of viral glycoproteins in transfected polarized epithelial cells. *J. Cell Biol.* 102:1242–1255.
18. Haas, I. G., and M. Wabl. 1983. Immunoglobulin heavy chain binding protein. *Nature (Lond.).* 306:387–389.
19. Hemmingsen, S. M., C. Woolford, S. M. van der Vies, K. Tilly, D. T. Dennis, C. P. Georgopoulos, R. W. Hendrix, and R. J. Ellis. 1988. Homologous plant and bacterial proteins chaperone oligomeric protein assembly. *Nature (Lond.).* 333:330–334.
20. Hendershot, L., D. Bole, G. Kohler, and J. F. Kearney. 1987. Assembly and secretion of heavy chains that do not associate posttranslationally with immunoglobulin heavy chain-binding protein. *J. Cell Biol.* 104: 761–767.
21. Hendershot, L. M., and J. F. Kearney. 1988. A role for human heavy chain binding protein in the developmental regulation of immunoglobulin transport. *Mol. Immunol.* 25:585–595.
22. Hendershot, L. M., J. Ting, and A. S. Lee. 1988. Identity of the immunoglobulin heavy-chain binding protein with the 78,000-dalton glucose regulated protein and the role of posttranslational modifications in its binding function. *Mol. Cell Biol.* 8:4250–4256.
23. Hiebert, S. W., and R. A. Lamb. 1988. Cell surface expression of glycosylated, nonglycosylated, and truncated forms of a cytoplasmic protein pyruvate kinase. *J. Cell Biol.* 107:865–876.
24. Hiebert, S. W., R. G. Paterson, and R. A. Lamb. 1985. Hemagglutinin-neuraminidase protein of the paramyxovirus simian virus 5: nucleotide sequence of the mRNA predicts an N-terminal membrane anchor. *J. Virol.* 54:1–6.
25. Kassenbrock, C. K., P. D. Garcia, P. Walter, and R. B. Kelly. 1988. Heavy-chain binding protein recognizes aberrant polypeptides translocated *in vitro*. *Nature (Lond.).* 333:90–93.
26. Kornfeld, R., and S. Kornfeld. 1985. Assembly of asparagine-linked oligosaccharides. *Annu. Rev. Biochem.* 54:631–664.
27. Kozutsumi, Y., M. Segal, K. Normington, M.-J. Gething, and J. Sambrook. 1988. The presence of malfolded proteins in the endoplasmic reticulum signals the induction of glucose-regulated proteins. *Nature (Lond.).* 332:462–464.
28. Kreis, T. E., and H. F. Lodish. 1986. Oligomerization is essential for transport of vesicular stomatitis viral glycoprotein to the cell surface. *Cell.* 46:929–937.
29. Lamb, R. A., and P. W. Choppin. 1976. Synthesis of influenza proteins in infected cells: translation of viral polypeptides, including three P polypeptides, from RNA produced by primary transcription. *Virology.* 74:504–519.
30. Lamb, R. A., P. R. Etkind, and P. W. Choppin. 1978. Evidence for a ninth influenza viral polypeptide. *Virology.* 91:60–78.
31. Lazarovits, J., and M. Roth. 1988. A single amino acid change in the cytoplasmic domain allows the influenza virus hemagglutinin to be endocytosed through coated pits. *Cell.* 53:743–752.
32. Lippincott-Schwartz, J., and D. M. Fambrough. 1987. Cycling of the integral membrane glycoprotein, LEP100, between plasma membrane and lysosomes: Kinetic and morphological analysis. *Cell.* 49:669–677.
33. Lodish, H. F., N. Kong, M. Snider, and G. J. A. M. Strous. 1983. Hepatoma secretory proteins migrate from rough endoplasmic reticulum to Golgi at characteristic rates. *Nature (Lond.).* 304:80–83.
34. Lodish, H. F. 1988. Transport of secretory and membrane glycoproteins from the rough endoplasmic reticulum to the Golgi. *J. Biol. Chem.* 263:2107–2110.
35. Machamer, C. E., R. Z. Florkiewicz, and J. K. Rose. 1985. A single N-linked oligosaccharide at either of the two normal sites is sufficient for transport of vesicular stomatitis virus G protein to the cell surface. *Mol. Cell Biol.* 5:3074–3083.
36. Markwell, M.-A. K., and F. Fox. 1980. Protein-protein interactions within paramyxoviruses identified by native disulfide bonding or reversible chemical cross-linking. *J. Virol.* 33:152–166.
37. Matlin, K., D. F. Bainton, M. Pesonen, D. Louvard, N. Genty, and K. Simons. 1983. Transepithelial transport of a viral membrane glycoprotein implanted into the apical membrane of Madin-Darby canine kidney cells. I. Morphological evidence. *J. Cell Biol.* 97:627–637.
38. Merion, M., and W. S. Sly. 1983. The role of intermediate vesicles in the adsorptive endocytosis and transport of ligand to lysosomes by human fibrobasts. *J. Cell Biol.* 96:644–650.
39. Merz, D. C., A. Scheid, and P. W. Choppin. 1980. Importance of antibodies to the fusion glycoprotein of paramyxoviruses in the prevention of spread of infection. *J. Exp. Med.* 151:275–288.
40. Merz, D. C., A. Scheid, and P. W. Choppin. 1981. Immunological studies of the functions of paramyxovirus glycoproteins. *Virology.* 109:94–105.
41. Morrison, T. G., and L. J. Ward. 1984. Intracellular processing of the vesicular stomatitis virus glycoprotein and the Newcastle disease virus hemagglutinin-neuraminidase glycoprotein. *Virus Res.* 1:225–239.
42. Mottet, G., A. Portner, and L. Roux. 1986. Drastic immunoreactivity changes between the immature and mature forms of the Sendai virus HN and F_0 glycoproteins. *J. Virol.* 59:132–141.
43. Munro, S., and H. R. B. Pelham. 1986. An HSP70-like protein in the ER: Identity with the 78 Kd glucose-regulated protein and immunoglobulin heavy chain binding protein. *Cell.* 46:291–300.
44. Munro, S., and H. R. B. Pelham. 1987. A C-terminal signal prevents the secretion of luminal ER proteins. *Cell.* 48:899–907.
45. Paterson, R. G., T. J. R. Harris, and R. A. Lamb. 1984. Fusion protein of the paramyxovirus simian virus 5: nucleotide sequence of mRNA predicts a highly hydrophobic glycoprotein. *Proc. Natl. Acad. Sci. USA.* 81:6706–6710.
46. Paterson, R. G., S. W. Hiebert, and R. A. Lamb. 1985. Expression at the cell surface of biologically active fusion and hemagglutinin/neuraminidase proteins of the paramyxovirus simian virus 5 from cloned cDNA. *Proc. Natl. Acad. Sci. USA.* 82:7520–7524.
47. Pelham, H. R. B. 1986. Speculations on the functions of the major heat-shock and glucose-regulated proteins. *Cell.* 46:959–961.
48. Pelham, H. R. B. 1988. Coming in from the cold (news and views). *Nature (Lond.).* 332:776–777.
49. Peluso, R. W., R. A. Lamb, and P. W. Choppin. 1977. Polypeptide synthesis in simian virus 5-infected cells. *J. Virol.* 23:177–187.
50. Peluso, R. W., R. A. Lamb, and P. W. Choppin. 1978. Infection with paramyxoviruses stimulates synthesis of cellular polypeptides that are also stimulated in cells transformed by Rous sarcoma virus or deprived of glucose. *Proc. Natl. Acad. Sci. USA.* 75:6120–6124.
51. Pesonen, M., and K. Simons. 1983. Transepithelial transport of viral membrane glycoprotein implanted into the apical plasma membrane of Madin-Darby canine kidney cells. II. Immunological quantitation. *J. Cell Biol.* 97:638–643.
52. Pfeffer, S. R., and J. E. Rothman. 1987. Biosynthetic protein transport and

sorting by the endoplasmic reticulum and Golgi. *Annu. Rev. Biochem.* 56:829–852.

53. Portner, A., and T. G. Morrison. 1990. Structure, function and intracellular processing of paramyxovirus glycoproteins. *In* The Paramyxoviruses. D. W. Kingsbury, editor. Plenum Publishing Corp., New York. In press.
54. Pouyssegur, J., R. P. C. Shiu, and I. Pastan. 1977. Induction of two transformation sensitive membrane polypeptides in normal fibroblasts by a block in glycosylation or glucose deprivation. *Cell.* 11:941–947.
55. Rademacher, T. W., R. B. Parekh, and R. A. Dwek. 1988. Glycobiology. *Annu. Rev. Biochem.* 57:785–838.
56. Randall, R. E., D. F. Young, K. K. A. Goswami, and W. C. Russell. 1987. Isolation and characterization of monoclonal antibodies to simian virus 5 and their use in revealing antigenic differences between human, canine and simian isolates. *J. Gen. Virol.* 68:2769–2780.
57. Rose, J. K., and R. W. Doms. 1988. Regulation of protein export from the endoplasmic reticulum. *Annu. Rev. Cell Biol.* 4:257–288.
58. Roth, M. G., C. Doyle, J. Sambrook, and M.-J. Gething. 1986. Heterologous transmembrane and cytoplasmic domains direct functional chimeric influenza virus hemagglutinins into the endocytic pathway. *J. Cell Biol.* 102:1271–1283.
59. Rothman, J. E. 1987. Protein sorting by selective retention in the endoplasmic reticulum and Golgi stack. *Cell.* 50:521–522.
60. Roux, L., P. Beffy, and A. Portner. 1985. Three variations in the cell surface expression of the haemagglutinin-neuraminidase glycoprotein of Sendai virus. *J. Gen. Virol.* 66:987–1000.
61. Scheid, A., L. A. Caliguiri, R. W. Compans, and P. W. Choppin. 1972. Isolation of paramyxovirus glycoproteins. Association of both hemagglutinating and neuraminidase activities with the large SV5 glycoprotein. *Virology.* 50:640–652.
62. Scheid, A., and P. W. Choppin. 1974. Identification of the biological activities of paramyxovirus glycoproteins. Activation of cell fusion, hemolysis, and infectivity by proteolytic cleavage of an inactive precursor protein of Sendai virus. *Virology.* 57:475–490.
63. Steinman, R. M., J. M. Silver, and Z. A. Cohn. 1983. Pinocytosis in fibroblasts. *J. Cell Biol.* 63:949–969.
64. Tartakoff, A. M. 1986. Temperature and energy dependence of secretory protein transport in the exocrine pancreas. *EMBO (Eur. Mol. Biol. Organ.) J.* 5:1477–1482.
65. Thompson, S. D., W. G. Laver, K. G. Murti, and A. Portner. 1988. Isolation of a biologically active soluble form of the hemagglutinin-neuraminidase protein of Sendai virus. *J. Virol.* 62:4653–4660.
66. Ting, J., and A. S. Lee. 1988. Human gene encoding the 78,000-Dalton glucose-regulated protein and its pseudogene: structure, function, and regulation. *DNA (NY).* 7:275–286.
67. Ting, J., S. K. Wooden, R. Kriz, K. Kelleher, R. J. Kaufman, and A. S. Lee. 1987. The nucleotide sequence encoding the hamster 78-kDa glucose-regulated protein (GRP78) and its conservation between hamster and rat. *Gene (Amst.).* 55:147–152.
68. Watanabe, N., H. Kuriyama, H. Sone, H. Neda, N. Yamauchi, M. Maeda, and Y. Niitsu. 1988. Continuous internalization of tumor necrosis factor receptors in a human myosarcoma cell line. *J. Biol. Chem.* 263:10262–10266.
69. Watowich, S. S., and R. I. Morimoto. 1988. Complex regulation of heat shock- and glucose-responsive genes in human cells. *Mol. Cell. Biol.* 8:393–405.
70. Waxham, M. N., D. C. Merz, and J. S. Wolinsky. 1986. Intracellular maturation of mumps virus hemagglutinin-neuraminidase glycoprotein: conformational changes detected with monoclonal antibodies. *J. Virol.* 59:392–400.
71. Wieland, F. T., M. L. Gleason, T. A. Serafini, and J. E. Rothman. 1987. The rate of bulk from the endoplasmic reticulum to the cell surface. *Cell.* 50:289–300.
72. Yewdell, J. W., A. Yellen, and T. Bachi. 1988. Monoclonal antibodies localize events in the folding, assembly, and intracellular transport of the influenza virus hemagglutinin glycoprotein. *Cell.* 52:843–852.